MARMARA UNIVERSITY

FACULTY OF ENGINEERING

Design and Analysis of Composite Panels with High Impact Resistance

Yusuf Çağrı Akay, Lukas Gevez, Seçkin Güler

GRADUATION PROJECT REPORT

Department of Mechanical Engineering

Supervisor

Prof. Dr. Bülent EKİCİ

ISTANBUL, 2023

MARMARA UNIVERSITY

FACULTY OF ENGINEERING

Design and Analysis of Composite Panels with High Impact Resistance

Yusuf Çağrı Akay(150418062)

Lukas Gevez(150418045)

Seçkin Güler(150418013)

GRADUATION PROJECT REPORT

Department of Mechanical Engineering

Supervisor

Prof. Dr. Bülent EKİCİ

ISTANBUL, 2023

MARMARA UNIVERSITY

FACULTY OF ENGINEERING

Design and Analysis of Composite Panels with High Impact Resistance

by

Yusuf Çağrı Akay, Lukas Gevez, Seçkin Güler

June 8, 2023, Istanbul

SUBMITTED TO THE DEPARTMENT OF MECHANICAL ENGINEERING IN PARTIAL FULFILLMENT OF THE REQUIREMENTS FOR THE DEGREE

OF

BACHELOR OF SCIENCE

AT

MARMARA UNIVERSITY

Signature of Author(s) .....Yusuf Çağrı AKAY, Lukas GEVEZ, Seçkin GÜLER

Department of Mechanical Engineering

Certified By .....Prof.Dr.Bülent EKİCİ

Project Supervisor, Department of Mechanical Engineering

Accepted By.....Prof.Dr.Bülent EKİCİ

Head of the Department of Mechanical Engineering

ACKNOWLEDGEMENT

Above all, we would like to thank our supervisor Prof. Dr. Bülent EKİCİ for the valuable guidance, sincerity, advice on preparing this thesis, giving us the vision for our future, and giving us moral and material support.

Also, we would like to thank Dr. Ali İmran AYTEN for his help and guidance through the manufacturing process and helping us tirelessly with every question we had. Also, thank you for donating the materials we needed manufacturing composites.

We also want to thank Dost Kimya A.Ş. for generously helping with our manufacturing materials. We are also grateful to Teijin Limited Company to supply Twaron CT709 fabric.

We would like to thank Semih ÖZKÜR from Istanbul Technical University for his help with drop tests.

Finally, we want to thank TUSAŞ for providing financial sources for this thesis.

July 2023 Yusuf Çağrı Akay, Lukas Gevez, Seçkin Güler

CONTENTS

ABSTRACT

Design and Optimization of Composite Panels with High Impact Resistance

This thesis focuses on the design and optimization of composite panels with enhanced impact resistance. The objective is to design a sandwich panel withstanding low-velocity impacts. Using aramid-epoxy composites.

To do so, investigation of papers including LVI tests, composite design and mechanical property determination is done.

The study employs a combination of computational modeling techniques and experimental testing. Computational modeling involves the design of the composite panel using SOLIDWORKS. Also, to increase the absorption capability of the panel, using biomimicry "scutoid" is used to design a new core shape. The design is done according to the requirements that are given as, 1mm top laminate thickness, 3mm core thickness and 0.5mm bottom ply thickness. With our Teijin CT709 aramid having an areal density of $200\ \mathrm{g/m^2}$, we can assume a ply number of 4 and 2 respectively for the composites. Next step includes the use of ANSYS Ls-Dyna. The digital experiments are designed using Taguchi arrays. Ply angles as parameters and angle possibilities as levels.

Experimental studies include the manufacturing of the composites, prepared by vacuum infusion and 3D printing of core region. The core sections are 3D printed using Ultimaker2 Extended printer. After the manufacturing the panels are cut to $15\mathrm{cm} \times 15\mathrm{cm}$ sections by water jet for assembly with epoxy and testing. In this study, all manufacturing is carried out at Marmara University by us. The drop tests are done by adjusting the initial energy as 150J to see the maximum energy absorbed and clarity of the graphs. The tests are carried out at Istanbul Technical University.

The test results show a trend of increase between plain composite, honeycomb sandwich, scutoid sandwich and aluminum plate, respectively. Scutoid core sandwich panel showed 20.92% increase in the energy absorption capability with respect to honeycomb core sandwich.

Keywords: Biomimicry, honeycomb, drop weight impact, low velocity impact, impact resistance.

SYMBOLS

E : Tensile modulus

E^* : Specific tensile modulus

E_{11} : Elastic modulus in the longitudinal direction

E_{22} : Elastic modulus in the transverse direction

E_{33} : Elastic modulus in the through-thickness direction

E_k : Kinetic energy

G_{12} : Shear modulus in 1-2 plane

G_{23} : Shear modulus in 2-3 plane

G_{31} : Shear modulus in 1-3 plane

h : Scutoid height

h_1 : Scutoid transition point height

l : Scutoid edge length

m_e : Epoxy mass fraction ratio

m_f : Fiber mass fraction ratio

m_i : Impactor mass

S_{11} : Shear strength in 1-2 plane

S_{23} : Shear strength in 2-3 plane

S_{31} : Shear strength in 1-3 plane

T_g : Glass transition temperature

T_m : Melting temperature

X_c : Compressive strength in the longitudinal direction.

$\mathbf{X_t}$ **:** Tensile strength in the longitudinal direction

$\mathbf{Y_c}$ **:** Compressive strength in the transverse direction

$\mathbf{Y_t}$ **:** Tensile strength in the transverse direction

$\mathbf{Z_c}$ **:** Compressive strength in the through-thickness direction

$\mathbf{Z_t}$ **:** Tensile strength in the through-thickness direction

$\boldsymbol{\varepsilon}$ **:** Ultimate strain

$\boldsymbol{\nu_{12}}$ **:** Poisson's ratio in 1-2 Plane

$\boldsymbol{\nu_{23}}$ **:** Poisson's ratio in 2-3 Plane

$\boldsymbol{\nu_{31}}$ **:** Poisson's ratio in 1-3 Plane

$\boldsymbol{\rho}$ **:** Density

$\boldsymbol{\sigma^*}$ **:** Specific tensile strength

$\boldsymbol{\sigma}$ **:** Tensile strength

ABBREVIATIONS

LVI **:** Low Velocity Impact

VARTM **:** Vacuum Assisted Resin Transfer Molding

ASTM **:** American Society for Testing and Materials

DWI **:** Drop Weight Impact

PLA **:** Polylactic Acid

LIST OF FIGURES

PAGE

LIST OF TABLES

PAGE

1 INTRODUCTION

In engineering, materials and their properties affect many aspects of a design. With this fact and the technology race in the world led the scientist into discovering new materials and techniques to improve performance of materials which might be specified by less weight, lower cost, less corrosivity and more strength, this might be against impact. Composites are a great example, because they are made of a different type of element from what they generally replace in aerospace, being metals (Matthews & Rawlings, 1994).

Composite materials offer several benefits over conventional engineering materials like aluminum and steel. Some of them being greater in strength and stiffness, better resistance to corrosion, and improved fatigue properties. Additionally, using fiber-reinforced plastic to manufacture components can often be more cost-effective than using traditional metals. Despite their benefits, composites have certain limitations. One of the most significant limitations is how they respond to localized impact loading such as runway debris, dropped tool as such (Cantwell & Morton, 1991). We can think of these situations being as low velocity impacts.

One of the aspects mentioned is the main topic of this project, which is the impact resistance. The goal of this study is to design a composite panel with specified thicknesses using computational methods, then manufacturing, and testing the low velocity impact performance of the panel. The aim is to give information about the impact resistance, design steps, materials, and methods in manufacturing of composites. We wanted to come up with a new core geometry using biomimicry, a recently discovered geometrical shape called ‘scutoid’ (Dhari & Patel, 2021). We also wanted to compare our results with traditionally used honeycomb core geometry. The core geometries were 3-D printed via Ultimaker 2 Extended machinery and we manufactured our composite panels with the results we got from our ANSYS Ls-Dyna analyses, which we did for honeycomb core composite panel to find the optimum angles for absorbing impact energy. After the assembly we conducted a low velocity impact test for both honeycomb and scutoid sandwich panel.

Aim of this study is to develop a composite panel with high impact resistance. The panel is required to have 1mm top laminate, 3mm core, 0.5mm bottom laminate thicknesses. Study aims to increase the ability to absorb energy by a core that is using biomimicry. Numerical and experimental tests were performed simultaneously, both the accuracy of the methods used, and the level of improvements made were examined.

1.1 Impact Studies of Composites in the Literature

Serge Abrate reviewed more than 285 articles that were published before 1989. Serge's article presents a comprehensive review of the literature on impact of laminated composites, considering both experimental and analytical approaches (Abrate, 1991).

Serge Abrate, reviewed more than 300 articles and most of these articles were published after 1989. This article showed that the impact strength of laminated composites has started to be an active area of research. Also, this paper showed that, at these times, most of researchers focused on low velocity impact damage (Abrate, 1994).

Anderson and Madenci's study present the results of an experimental investigation concerning the low-velocity impact response of sandwich composites. Impact tests were conducted to characterize the type and extent of the damage observed in a variety of sandwich configurations with graphite/epoxy face sheets and foam or honeycomb cores. Correlation of the residual indentation and cross-sectional views of the impacted specimens provide a criterion for the extent of the damage. In the foam-core samples, significant damage was found to be present for residual indentations over 0.13 mm. Although the high-density foam-core and thicker face sheet increased the amount of energy required to generate damage, the damage was still similar for similar levels of residual indentation. For the honeycomb samples, 0.25 mm of residual indentation indicated significant levels of internal damage. However, the surfaces of both the honeycomb and foam samples revealed very little damage at these levels of impact energy. As the impact energy was increased, the samples experienced one of two types of damage: a tear or crack from the center of the laminate to the edge, or significant damage consisting of a dent localized in the region of impact (Anderson & Madenci, 2000).

Naik worked on the behavior of woven fabric laminated composite plates under transverse central low velocity point impact by using a modified Hertz law and 3D transient finite element analysis code. It is observed that the in-plane failure function is lower for woven-fabric laminates than for cross ply laminates, indicating that woven-fabric laminates are more resistant to impact damage (Naik, Sekher, & Meduri, 2000).

Hosur and Abdullah's study, experimental investigations were carried out to determine the response of four different combinations of hybrid laminates to low-velocity impact loading using an instrumented impact testing machine. Hybrid laminates were fabricated with twill weave carbon fabric and plain weave S2-glass fabric using vacuum assisted resin molding

process with SC-15 epoxy resin system. Response of carbon/epoxy and glass/epoxy laminates was also investigated to compare with that of hybrid samples. Square laminates of size 100 mm and nominal thickness of 3 mm were subjected to low-velocity impact loading at four energy levels of 10, 20, 30 and 40 J. Results of the study indicate that there is considerable improvement in the load carrying capability of hybrid composites as compared to carbon/epoxy laminates with slight reduction in stiffness (Hosur, Abdullah, & Jeelani, 2005).

Donadon studied on progressive failure model for composite laminates subjected to low velocity impact damage. Article presents a 3-D failure model for predicting the dynamic material response of composite laminates under impact loading. The formulation is based on the Continuum Damage Mechanics (CDM) approach and enables the control of the energy dissipation associated with each failure mode regardless of mesh refinement and fracture plane orientation. Internal thermodynamically irreversible damage variables were defined in order to quantify damage concentration associated with each possible failure mode and predict the gradual stiffness reduction during the impact damage process. The material model has been implemented into LS-DYNA explicit finite element code within solid elements and it has proven to be capable of reproducing experimental results with good accuracy in terms of static/dynamic responses, absorbed energy and extent of damage (Donadon, Ianucci, Falzon, Hodgkinson, & Almeida, 2008).

Tita studied failure analysis of low velocity impact on thin composite laminates. They investigated the influence of stacking sequence and energy impact using load time histories, displacement time histories and energy time histories as well as images from NDE. Indentation tests results were compared to dynamic results, verifying the inertia effects when thin composite laminate was impacted by foreign object with low velocity. Finite element analysis (FEA) was developed, using Hill's model and material models implemented by UMAT (User Material Subroutine) into software ABAQUS™, in order to simulate the failure mechanisms under indentation tests (Tita, Carvalho, & Vandepitte, 2008).

Rajesh and Jerald studied how woven glass fiber composites with an epoxy matrix respond to low velocity impact using ASTM standards with a drop weight machine. They located the response and location of damage at impact velocities between 2 and 4.5 m/s and with energy levels between 3 and 15 J. They noticed a disastrous laminate response at 4.429 m/s. They discovered that failure is either from cracking or laminate perforation (Mathivanan &

Jerald, 2010).

Shi and Swait worked on modelling damage evolution in composite laminates subjected to low velocity impact. They described nonlinear shear behavior of composite by using Soutis shear stress-strain semi empirical formula. They employed finite element method to simulate the behavior of composite under low velocity impact. Interface cohesive elements were inserted between plies with appropriate mixed-mode damage laws to model delamination. Their damage model was implemented in the FE code (Abaqus/Explicit) by a user-defined material subroutine (VUMAT). Their numerical results in general gave a good agreement compared to experimentally obtained curves of impact force and absorbed energy versus time. The various damage mechanisms introduced during the impact event were observed by non-destructive technique X-ray radiography and were successfully captured numerically by the proposed damage evolution model (Shi, Swait, & Soutis, 2012).

Grunenfelder et al worked on bio-inspired impact-resistant composites. They applied helicoidal design strategy to fabrication of high-performance carbon fiber-epoxy composites. Through experimental and computational methods, a helicoidal architecture is shown to reduce through-thickness damage propagation in a composite panel during an impact event and result in an increase in toughness. Their findings have implications in the design of composite parts for aerospace, automotive and armor applications (L K Grunenfelder, et al., 2014).

Li investigated experimentally on the impact behavior of pultruded composites samples subjected to low-velocity impacts with higher impact energies ranging from 16.75 to 67 J. The specimens were placed and supported according to the requirement of ASTM 7136 standard. Their results of impact characteristics and performance are demonstrated and compared for different impact energy levels. The damage evaluation is also introduced to compare the failure modes of pultruded composites subjected to different energy levels. The development and propagation of stress during the low velocity impacts are analyzed using the finite element method. Their numerical predictions were found to corroborate the experimental results in terms of load-time and central deflection-time curves (Li, Khennane, P, & Brown, 2017).

Dogan and Arikan studied an experiment on impact response of sandwich composite panels with thermoplastic and thermoset face-sheet. E-glass reinforced epoxy (thermoset) and polypropylene(thermoplastic) have been used to produce polymer composite face-sheets

and PVC foam was used as a core material. Several low velocity impact tests were performed under various impact energies. Besides the individual impact behavior of the thermosets and thermoplastic sandwich composites, the impact response of sandwich composites having hybrid sequences was also investigated. Their study showed that sandwich composites must have the harmony between core and the face sheet material. The deformation required for core densification must be able to compensate by the face sheet material (Dogan & Arikan, 2017).

He's and Yao's research focused on the low-velocity impact response and resulting damage behavior of aluminum honeycomb sandwich structures with carbon fiber reinforced plastic (CFRP) face sheets by combining the experimental and numerical methods. Low-velocity impact tests are conducted to determine and quantify the effects of structural parameters, such as face sheet thickness, cell wall thickness, honeycomb core height and hexagon side length, on the impact load, energy absorption, and failure mode. They performed numerical simulation to characterize the impact response and explore the deformation/failure mechanisms. Their predicted impact load, energy absorption, contact time and failure mode agreed well with measured counterparts. Their studies reveal that face sheet thickness has a particularly significant influence on the impact resistance performance of honeycomb structures. Their studies show that cell wall thickness and side length of honeycomb core have notable effect on the impact load and structural stiffness of such structures, while which do not play a great role in energy absorption. Increase in core height has comparatively little effect on initial stiffness and energy absorption but makes the second peak loads decreasing for the perforation cases (He, et al., 2019).

Zhang's and Xu's research presents the the low-velocity impact behavior of sandwich panel with carbon fiber reinforced plastic (CFRP) composite face sheet and Nomex honeycomb core through experimental and numerical methods. Experiments were carried out on two thicknesses of honeycomb core at various impact energy levels. The damage modes were obtained through non-destruction inspection (NDI) C-scan and microscopic observation. A refined three-dimensional finite element model combined with continuum damage mechanics (CDM) was developed with composite plies and detailed honeycomb core. Physically-based Puck's composite failure criteria and energy based progressive damage model were used to capture the intralaminar damage initiation and evolution, respectively. The interlaminar damage of facesheet and debonding of facesheet/core interface were predicted using cohesive element. The hexagonal honeycomb cells were characterized in

FE model with an elasto-plastic constitutive model and damage criterion in detail during impact. Their simulation results show good agreements with experiments and thier model can be used to predict the low-velocity impact response and impact damage effectively (Zhang, Xu, Zang, & Feng, 2020).

Usta and Türkmen described the low-velocity impact behavior of composite sandwich panels with different types of auxetic (negative Poisson's ratio) and non-auxetic prismatic core structures. They manufactured sandwich panels with carbon/fiber epoxy composite face sheets, polyurethane rigid foam core or 3D printed PLA plastic cellular honeycombs head (hexagonal, re-entrant, hexachiral and arrowhead). They determined material properties of the constituents via tensile and compression tests. A rigid striker with a hemispherical head tip is dropped on the specimens with a speed of 2.6 m/s. Their explicit finite element (FE) models are validated by the experimental results. Their work's results show that non-auxetic cores could have advantages over the auxetic ones at small deformation (impact energy is equal to 10 J) due to the larger contact surface and higher thickness of the cellular structure. Also they show that the auxetic core, provides greater impact resistance and energy absorption capability as the impact energy increases due to the larger densification and lower indentation during collapse. As a result, the arrowhead and hexachiral configurations are those mostly recommended for applications involving impacts under large deformations (Usta, Türkmen, & Scarba, 2021).

2 MATERIALS and METHOD

2.1 Materials

In this study, Twaron CT709 plain weave woven fabric which has an areal density of 200g/m^2 was used. Araldite LY1564 was the epoxy resin and Aradur 3486 was the hardener. PLA was used for the honeycomb and scutoid geometry core which has a density of 1.24 g/cm^3. For 100g of epoxy resin 34g hardener was used.

Table 2.1. Physical properties of the epoxy resin **(Huntsman, 2012)**.

Araldite LY1564	
Viscosity at 25 °C (mPa s)	1200 - 1400
Density at 25 °C (g/cm^3)	1.1 - 1.2
Epoxy index (Eq/kg)	5.8 - 6.05

Table 2.2. Physical properties of the hardener **(Huntsman, 2012)**.

Aradur 3486	
Viscosity at 25 °C (mPa s)	10 - 20
Density at 25 °C (g/cm^3)	0.94 - 0.95
Amine Value (Eq/kg)	8.55 - 9.30

2.2 Optimization Method

2.2.1 Design Guidelines for Composites

To design composite laminate, we firstly select our ply angles to fit our application which is impact damage. Because of manufacturing limitations, the fundamental angles that are used for ply orientations are $0°, \pm 15°, \pm 30°, \pm 45°, \pm 60°, \pm 75°, 90°$. Due to time and resources limitation, we could not try every combination, instead of this we select our angles with respect to laminate design guidelines.

1) Symmetry. Whenever possible, stacking sequences should be symmetric about mid-plane.
2) Balance. Whenever possible, stacking sequences should be balanced, with the same number of $+\theta^o$ and $-\theta°$ plies ($\theta \neq 90°$ and $\theta \neq 0°$).
3) Contiguity. No more than given number of plies of the same orientation should be stacked together. The limit is set here to two plies.
4) Disorientation. The difference between the orientations of two consecutive plies should not exceed 45^o.

5) A minimum of 10% of plies in each of the $0°, \pm 45°, 90°$ directions is required.

These laminate design guidelines are considered as a basis for the design of the stacking sequences of most composite structures in the aerospace industry (Irisarri, Lasseigne, Leroy, & Le Riche, 2014).

2.2.2 Design of Experiments via Taguchi Method

The Taguchi method, developed by Dr. Genichi Taguchi (Taguchi, 1990), is a technique for determining the optimum combinations of the process conditions widely employed in engineering analysis and the world of manufacturing. Taguchi method is a very powerful tool for designing and improving high-quality systems. By utilizing the Taguchi method, the industries can greatly reduce the time of product development without any sacrifice on the cost (Ross, 1995).

The Taguchi method is created with arrays. In these arrays, columns are called levels and rows called parameters. These matrices make it possible to the design a minimum number of experiments while still capturing the effect of various parameters combinations.

Various combinations of ply angles inside the composite affect the energy absorption ability of composite. In this research, one of our goals was to find the most energy absorbing combination of plies. With respect to design guidelines, we determined the number of levels and parameters for the Taguchi Method. Our parameters were the number of layers of composite, which is six, levels are the angles which is four. With these values, we had to do 4^6 trials to find best combination. To minimize this value, we chose to apply the Taguchi Method.

It is important to lower the number of parameters to get better results for optimization methods (Mach, 2015). This can be done by connecting parameters to each other. To do so what we did was to follow composite design guidelines. According to our physical constraints we are to have 4 and 2 levels of plies on top and bottom laminates respectively. Using the symmetry constraint on design, using bottom ply angle, first top ply and second top ply angle we were able to lower the parameter number from 6 to 3. Then the following Taguchi array is constructed using MINITAB.

Table 2.3. Initial Taguchi array

Bot	Top 1	Top 2
-45	-45	-45
-45	0	0
-45	45	45
-45	90	90
0	0	-45
0	-45	0
0	90	45
0	45	90
45	45	-45
45	90	0
45	-45	45
45	0	90
90	90	-45
90	45	0
90	0	45
90	-45	90

Using this array, we constructed a new one to conduct our experiments.

Table 2.4. Edited Taguchi array

Bot 1	Bot 2	Top 1	Top 2	Top 3	Top 4
-45	-45	-45	-45	-45	-45
-45	-45	0	0	0	0
-45	-45	45	45	45	45
-45	-45	90	90	90	90
0	0	0	-45	-45	0
0	0	-45	0	0	-45
0	0	90	45	45	90
0	0	45	90	90	45
45	45	45	-45	-45	45
45	45	90	0	0	90
45	45	-45	45	45	-45
45	45	0	90	90	0
90	90	90	-45	-45	90
90	90	45	0	0	45
90	90	0	45	45	0
90	90	-45	90	90	-45

The grayed columns are the ones generated.

2.3 Numerical Studies

2.3.1 Low Velocity Impact Simulations

LVI simulations were run on a honeycomb core composite to foresee the performances of possible composite panels and select the best performing composite in order to design an impact absorbing composite panel. Consequentially with the results and the angles of the panel we have we will run experimental tests on honeycomb core and also with our new core type we call scucomb. This will enable us to understand the validity of our simulation method and give knowledge about the performance comparison of honeycomb and scucomb core sandwich panels.

Impactor in the simulation is modelled according to ASTM D7136 DWI (ASTM, 2020). What we are simulating is a ball of 1.6cm in diameter being hit to our composite in the mid-point. To do so our first approach was to use ANSYS ACP and optimization modules. Our model in ACP was no compatible with the dynamic analysis modules. Our second approach was to use Ls-Dyna by itself. At first, we encountered some problems with the solver. We learned that Ls-Dyna is not very fond of face-to-face and edge-to-face contacts. But our model was consisting solid bodies in the first place. To overcome this problem we modeled, and assembled our geometry with surfaces only, after doing so in our assembled geometry we imprinted our core geometry to the surfaces at top and bottom, then we connected the composites to the core with Joint command. This operation allowed us to have connection of our finite element nodes between core and composite panels. After the operation showed us 16249 connections between.

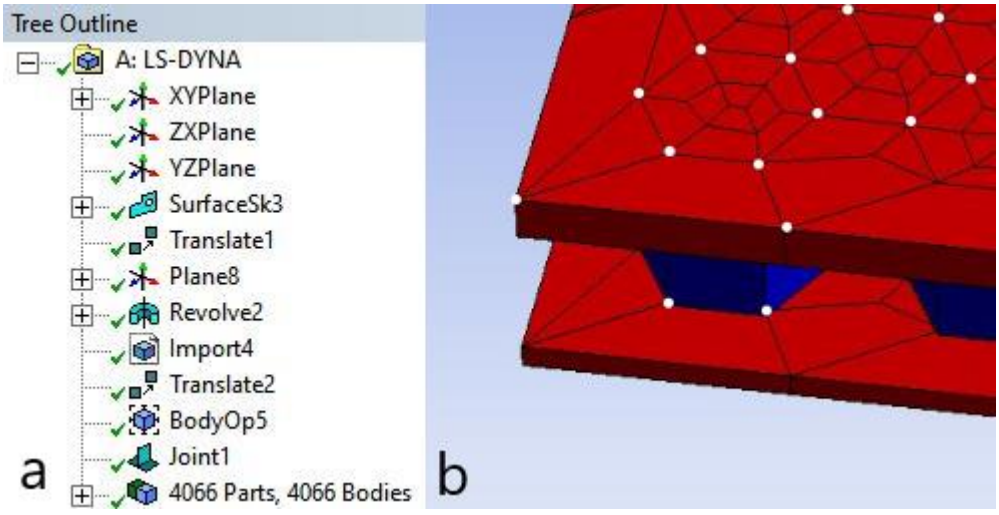

Figure 2.1. a) Tree Outline of Model, b) Merged nodes highlighted with white dots

Mesh size in the honeycomb design for the composite and core is 6mm and for the impactor

it is 3mm. There are two reasons for the use of mesh sizing for the impactor, firstly if we use bigger size mesh, the elements create sharp edges creating a stress concentration point on the impacted object. Second, it increases the accuracy for the kinetic energy calculation of the impactor. Lastly, we also lowered the size of the mesh for the composite, this is to avoid hourglassing. It is seen that big meshes cause the rise in hourglass energy.

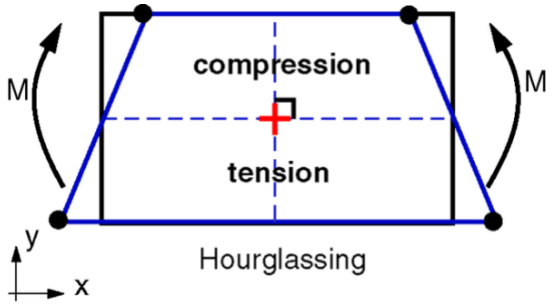

Figure 2.2. Hourglassing in four node element.

This happens when analyzer uses reduced integration element. This problem happens because these elements have only one integration point (in the middle). This way the program can't detect strain. Element deforms but since there is no strain, there is no strain energy.

Then we added the connection under the mesh tree branch as node merge group. We imported our model and in model we added layered sections and selected the top and bottom surfaces separately into two different layered sections. Then constructed series of experiments in this manner. Also, as we discussed our core geometry is now made of surfaces, we entered a generally used thickness value of 0.4mm for our honeycomb core.

Nodes	41128
Elements	47828

Figure 2.3. Node and element number for the honeycomb simulations.

For the initial conditions and constraints, we allowed the impactor to only be free in the z direction. We forbid the rotation of it as well, since in the test bench it is also not allowed. Also, to make the reading of our results easier we wanted to pierce through the composite and have a clear graph with our panel absorbing the maximum energy that it can. Since we are trying to have our impactor to be constrained within $10\ m/s$ impact speed, and not to have any other geometry in the simulation making it harder to solve we gradually increased our density to be high enough to pierce through our composite panel. We appointed an initial velocity in in z-direction vectorially to our impactor also fixing the edges of our composites and the side faces of our core geometry.

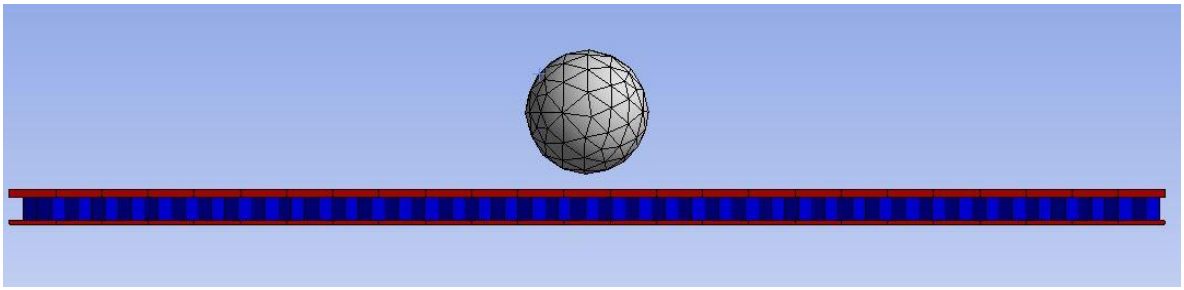

Figure 2.4. Side-view of simulation

Due to the complexity of the geometry, other than scutoid simulations, all simulations were run on a desktop computer with Intel i7-3770 processor, 12 gb RAM.

Material properties for the composite are shown in the below table (Ayten, 2020).

Table 2.5. Material properties of aramid epoxy composite used in the ANSYS.

Property	Value
ρ (kg/m3)	1440
E_{11} (MPa)	10130
E_{22} (MPa)	10130
E_{33} (MPa)	6066
G_{12} (MPa)	1530
G_{23} (MPa)	916
G_{31} (MPa)	916
ν_{12}	0.154
ν_{23}	0.092
ν_{31}	0.092
X_t (MPa)	577
Y_t (MPa)	577
X_c (MPa)	110
Y_c (MPa)	110
Z_t (MPa)	345
Z_c (MPa)	66
S_{12} (MPa)	125
S_{23} (MPa)	75
S_{31} (MPa)	75

Material properties for the PLA are displayed in below table (Farah, Anderson, & Langer, 2016).

Table 2.6. Material Properties of PLA used in ANSYS.

Properties	Value
$\rho(g/cm^3)$	1.21-1.25
σ (MPa)	21-60
E (GPa)	0.35-3.5
ε (%)	2.5-6

σ^* (Nm/g)	16.8-48
E^* (kNm/g)	0.28-2.8
T_g (°C)	45-60
T_m (°C)	150-162

The simulations were run according to the angles we found with Taguchi Optimization.

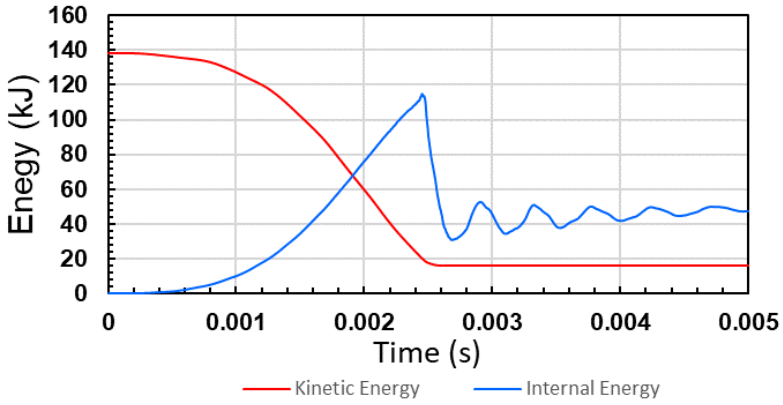

Figure 2.5. Results of the best performing honeycomb sandwich panel.

The results are displayed in the Table 2.7. The reading of the graphs is done with the subtraction of kinetic energy differences of the impactor.

Table 2.7. Results of numerical experiments done by Ls-Dyna

Experiment#	Bot2(°)	Bot1(°)	Top1(°)	Top2(°)	Top3(°)	Top4(°)	Energy Absorbed (J)
1	-45	-45	-45	-45	-45	-45	97,5
2	-45	-45	0	0	0	0	106
3	-45	-45	45	45	45	45	93,1
4	-45	-45	90	90	90	90	83,4
5	0	0	0	-45	-45	0	92,3
6	0	0	-45	0	0	-45	107
7	0	0	90	45	45	90	105
8	0	0	45	90	90	45	86,1
9	45	45	45	-45	-45	45	94
10	45	45	90	0	0	90	109
11	45	45	-45	45	45	-45	89
12	45	45	0	90	90	0	108
13	90	90	90	-45	-45	90	108
14	90	90	45	0	0	45	88,7
15	90	90	0	45	45	0	115
16	90	90	-45	90	90	-45	82,2

As can be seen on the Table 2.7, sandwich panel with $[90]_s$ and $[0/45]_s$ composite panels absorbed 115kJ of energy. Due to the time and computational power requirement of the

scutoid analysis, it is only run with the specified laminates.

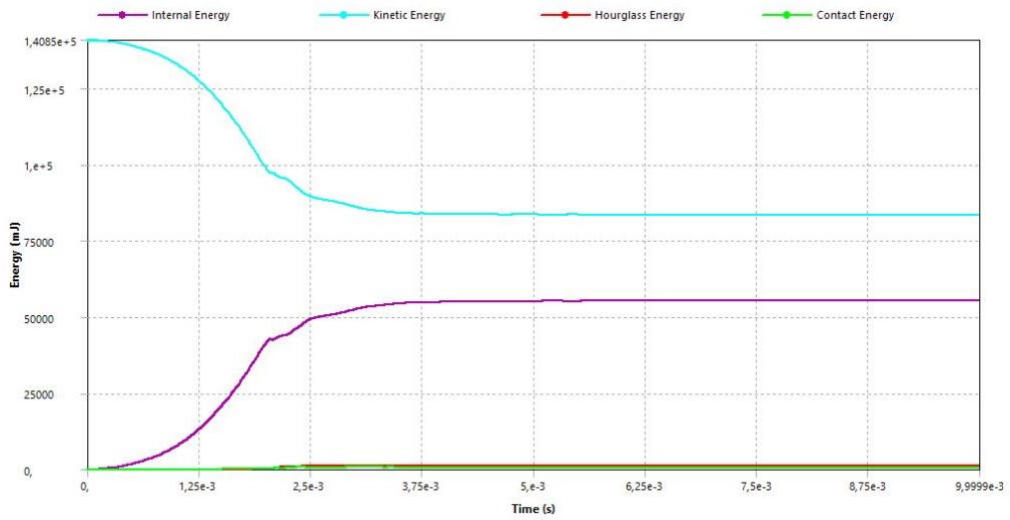

Figure 2.6. Energy graph for the scutoid simulation taken from ANSYS.

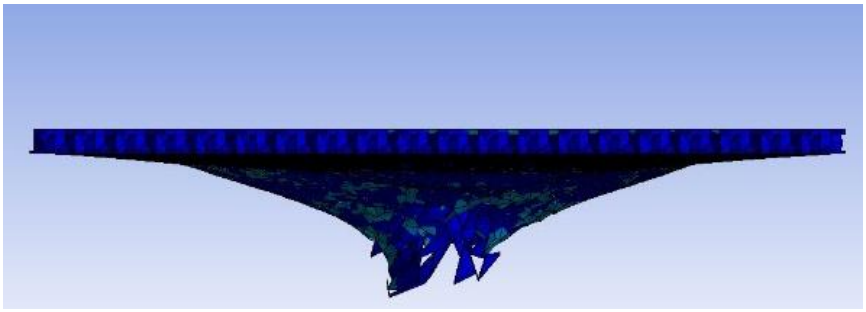

Figure 2.7. After impact image of scutoid core sandwich panel.

The difference in the results is assumed to be due to different modelling technique done on the scutoid due to the complex nature of it.

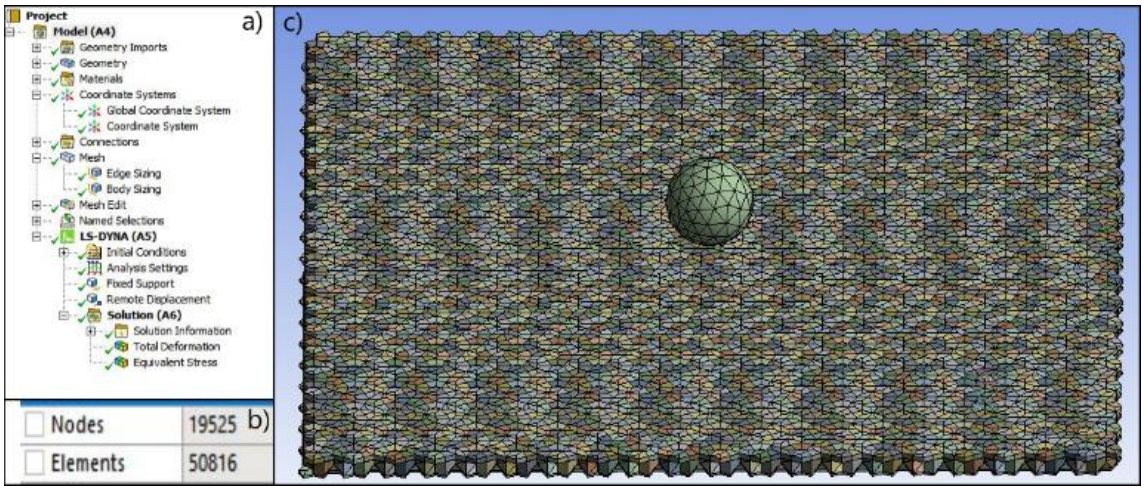

Figure 2.8. a) Scutoid simulation project tree. b) Node and element number of scutoid analysis. c) Mesh view of the simulation

To setup the scutoid simulation, model is generated as follows.

- On top of the scutoid core, set of surfaces are generated from edges.
- These surfaces are multiplied by pattern function in design modeler.
- Using BodyOp, the surfaces are sewed together. Then mirrored about the midpoint of core.
- Then using joint function core and surfaces are connected.

2.4 Experimental Studies

2.4.1 Scutoid core design

The epithelial tissues are found in the surfaces of organs and living beings. The tissues consist of various geometrical shapes such as cuboids, columnar or squamous cells joins together to form sheets which constitute the covering of an organic body. These cells may have a single or multilayer arrangement to form as sheets based on the organism. These sheets are observed to have an astounding set of behaviors under stresses. The sheets can be elongated, compressed, or bent of shape to form different structures. The sheets connected provide mechanical stability and act as barriers for different segments of an organ. The apical (top) surface of the sheet is exposed to air or liquid towards the outside of the organism whereas its counterpart, the basal (bottom) surface remains connected to the basement membrane. Gomez-Galvez et al. discusses the possible prism shapes of the epithelial cells with polygonal apical and basal faces. The study employed mathematical modelling to unveil a novel shape termed as ‘Scutoid’. The Scutoid is said to have formed because of the fundamental reorganization of cells along the apico-basal axes. The name of the shape is inspired by the likeness of a thorax of beetles (Dhari & Patel, 2021).

One of the most important goals of this project is to optimize the geometry called Scutoid and use it as a core in Sandwich panel models.

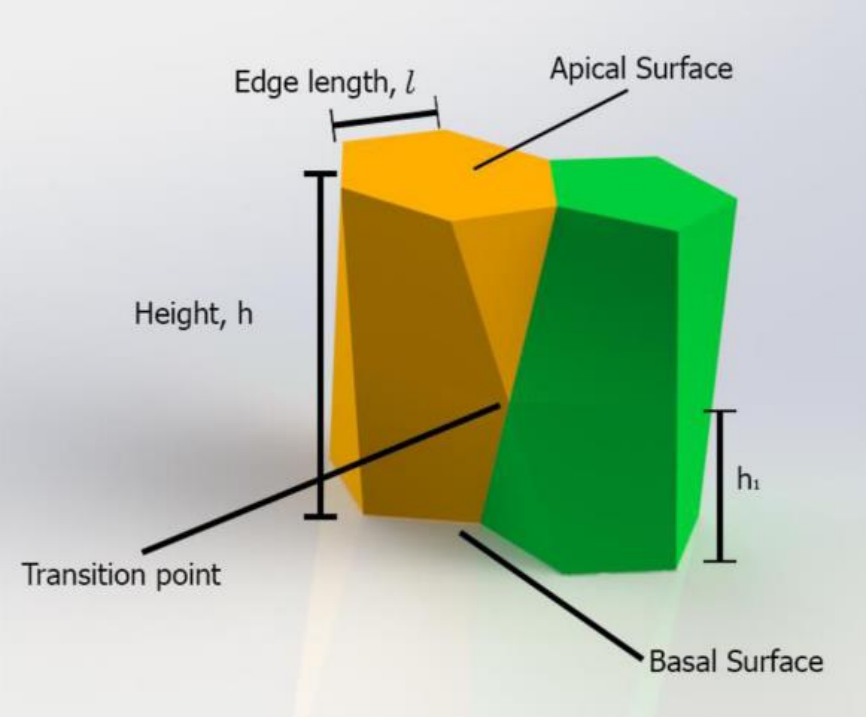

Figure 2.9. Self-Packing Scutoid **(Dhari & Patel, 2021)**.

Self-packing scutoid, one of the most popular scutoid types shown in Figure 2.9, is not a suitable model for core building because it can only be stacked in dual structures. In order to achieve our goal, we decided to design a scutoid model that can be stacked infinitely. Before creating our scutoid model, we decided to analyze the reasons why the self-packing scutoid can only be stacked dual and to find solutions on these reasons. As a result of our observations, we observed that the dual structuring is mainly due to 2 reasons:

- As the first reason, when the scutoid in Figure 2.9 was examined, we observed that the scutoid contains 1 transition point. Considering the combination of scutoids from transition points while stacking, we decided to have 2 transition points in opposite directions in the model we will design to solve this problem.
- The second reason we observed is that the upper and lower faces of the self-packed scutoid are composed of hexagonal and pentagonal surfaces. In our experiments, we saw that it is very difficult for equilateral pentagonal and equilateral hexagonal surfaces to combine in a row and form a regular pattern without gaps, so we decided to use the same geometric shape on the upper and lower surfaces of the scutoid we will design. Considering the fact that there are 2 transition points in the opposite direction we mentioned in the first reason, we decided that the most suitable shape for us to meet these requirements should be equilateral pentagon.

Together with these criteria, when we evaluated the boundary conditions that our TUSAS industry consultant Furkan KARABOĞA would consider during the design for us, we designed the scutoid model, the details of which are given below:

- As a result of the boundary conditions determined by our TUSAS industry consultant, Furkan KARABOĞA, we decided that the height (h) should be 3mm.
- Since we wanted the scutoid to have a rectangular skeleton, we set the edge length (l) as 2 mm.
- To facilitate unlimited stacking, we decided to have 2 transition points in opposite directions.
- Since we wanted it to be equidistant from the apical and basal surfaces, we decided to have the transition point height (h_1) of 1.5 mm.
- We decided that the surfaces should be equilateral pentagon as it patterned more easily and fit two transition point structures in opposite directions.

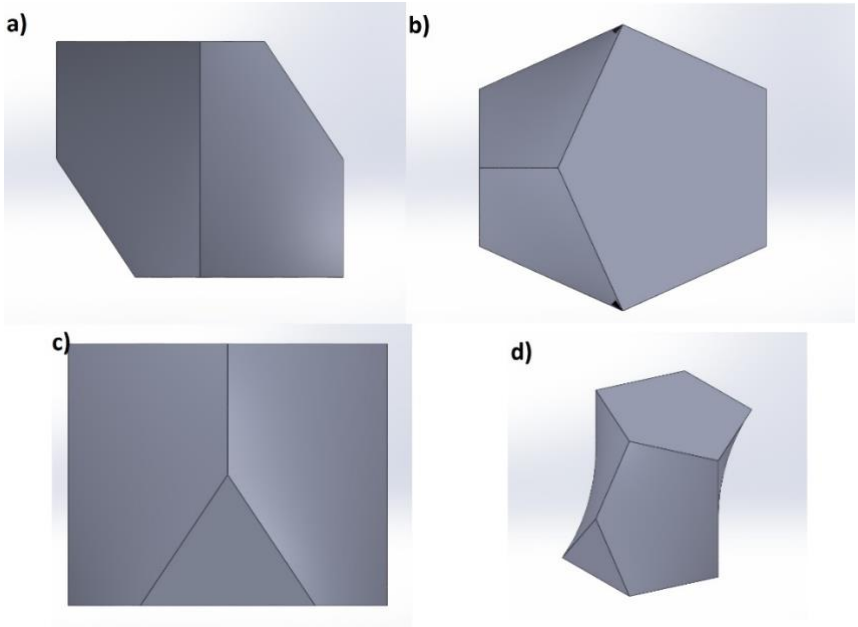

Figure 2.10. a) Front View, b) Top View, c) Right View, d) Isometric View

After the main scutoid design was finished, it was time for the core design. We arranged the model with a wall thickness of 0.2mm and created a core of 15cm x 15cm to comply with the boundary conditions set by our TUSAS industry consultant, Furkan KARABOĞA.

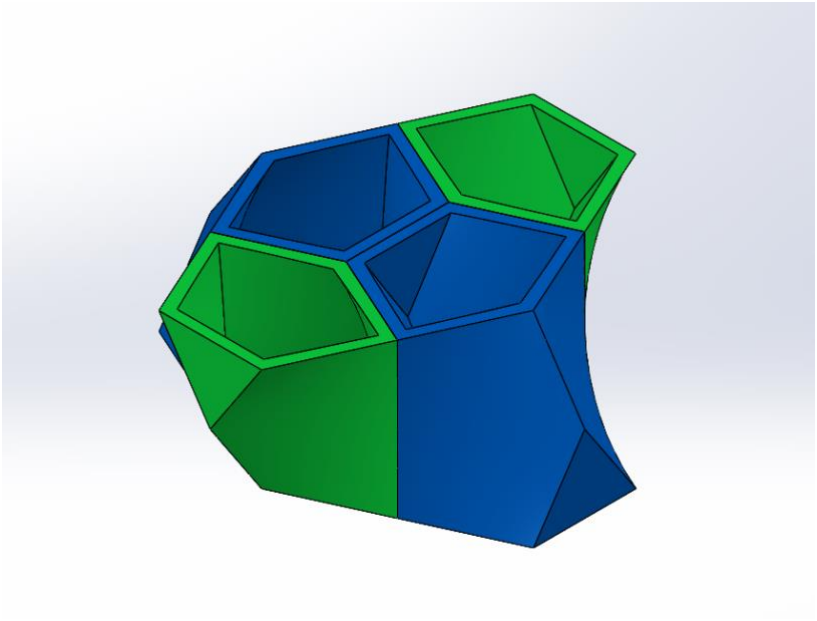

Figure 2.11. Quadruple Scutoid

An example stacking of four scutoids is shown in Figure 2.11. The remaining core, shown in Figure 2.12, was designed using these quadruple structures. After this step, the scutoid core design is completed.

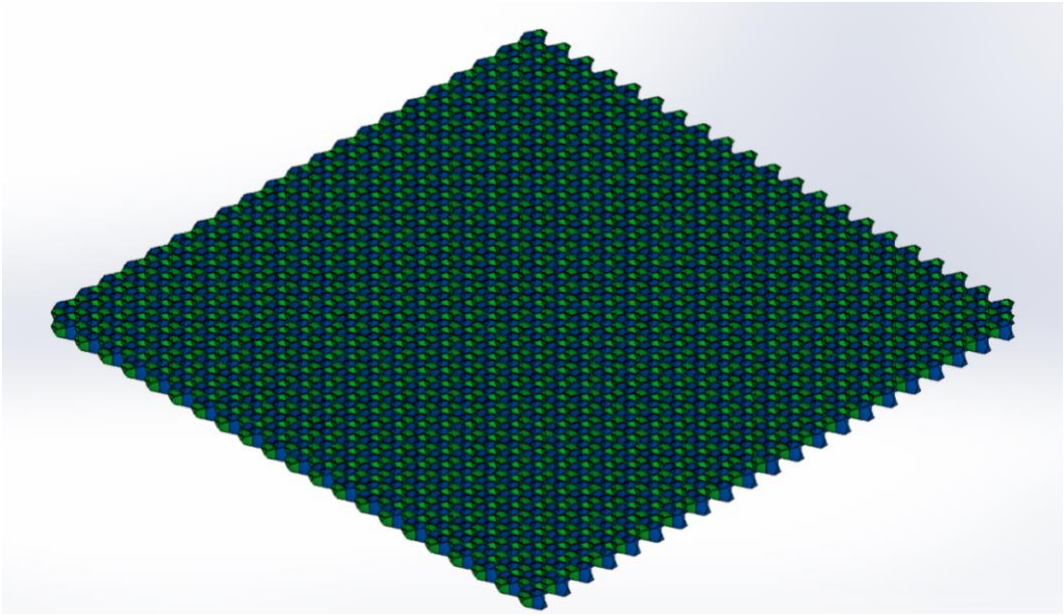

Figure 2.12. Scutoid Core

2.4.2 Honeycomb core design

As closely resembling the bee's honeycomb, scientists have found that the hexagonal structure performs excellent behavior with the largest usable space, showing a huge mechanical potential. The first artificial honeycomb structure was made with paper in China 2000 years ago. The manufacture of modern honeycomb products probably began in the

late 1930s. It was not until 1945 that the first all-aluminum sandwich panel was manufactured. Since then, kinds of cellular honeycomb structures were made from many different materials, such as the aluminum alloy, stainless steel, titanium, and the non-metallic materials. Sufficient attentions were attached on them, due to their outstanding energy absorption properties, light weight, and cost saving, not only for railway vehicle, automobile, subway, but also for airplane, ship and re-entry capsule of spacecraft etc (Wang, 2019).

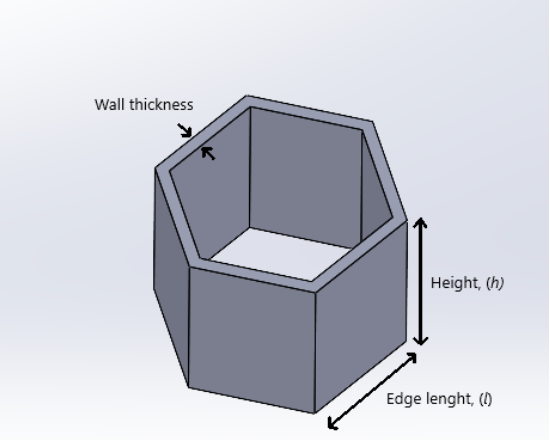

Figure 2.13. Single Honeycomb Geometry

Since it is already used in the aircraft industry, we decided to compare the geometry of the scutoid with the honeycomb. The same dimensions as the scutoid geometry were used when designing the honeycomb core to create equal conditions in finite element analyzes and drop tests. As a result:

- Honeycomb height at 3mm.
- Edge lengths were determined as 2mm.
- Wall thickness was determined as 0.2mm.

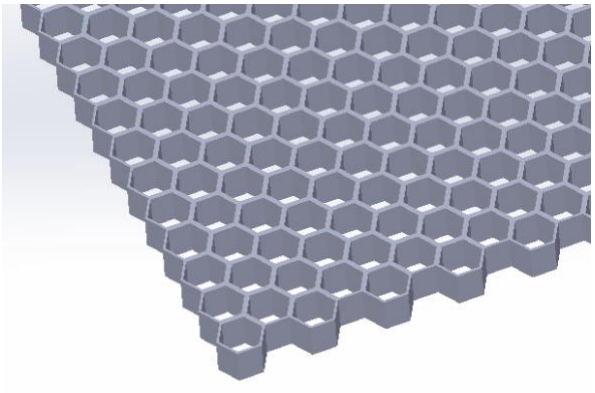

Figure 2.14 Honeycomb Core

2.4.3 Composite manufacturing and characterization

For the manufacturing of composite panels VARTM method was used. VARTM technique is versatile meaning that ideally it can be used to manufacture any size of composite because it does not require any special equipment like an oven. The fibers are stacked and wrapped with a vacuum bag and resin is drawn inside the bag to fill the gaps among the layers. (Beaumont, Constantinos, & Hodzic, 2015) The process consists of several steps, preparing the vacuum bag and lay-up, enclosing the vacuum bag and creating vacuum, resin preparation, resin infusion and finally the curing process.

According to the requirements given for the design of sandwich panel layup is given in the below figure.

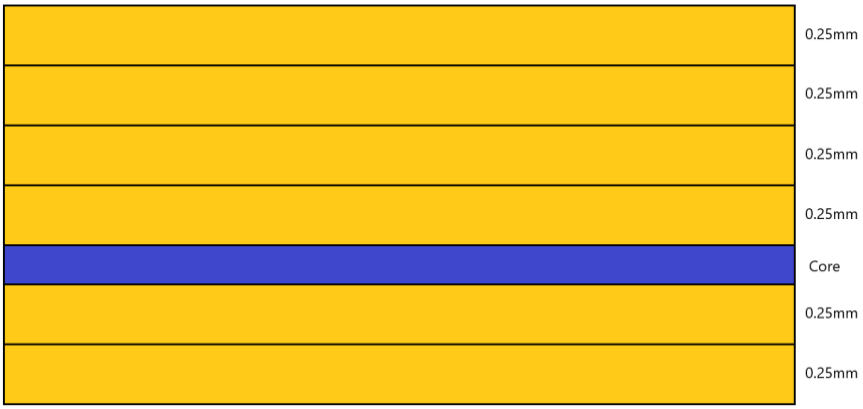

Figure 2.15. Sandwich panel layup

As two-ply bottom and four-ply top laminate the manufacturing has two phases. The fabrics we had were precut as $30\text{cm} \times 30\text{cm}$, to make the numerical tests and 3-D print of core geometry easier we selected our section as $15cm \times 15cm$. After the manufacturing we cut the composites with water jet. The release film is laid on the table and then two-sided adhesive tape is applied tracing the edge of the release film, bonding it to the table. Fabrics are aligned accordingly, then spiral pipes were placed to distribute the epoxy. Before enclosing the plies with vacuum bag, peel-ply and flow mesh are placed on top of the plies, ensuring ease of removal and infusion quality respectively. Figure 2.16 shows the VARTM method and its components that are used in manufacturing.

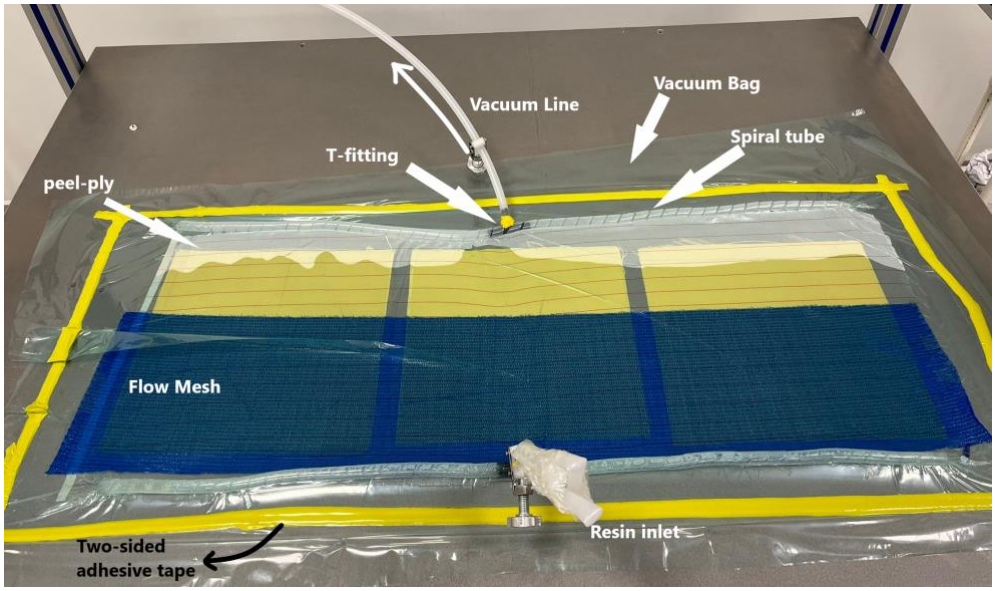

Figure 2.16. Vacuum infusion process and its components

After these steps, a test vacuum is done to see if there are any leaks. If there is a leak, firstly critical points need to be checked. If not one can move on to the resin preparation. System is left to cure for 24 hours.

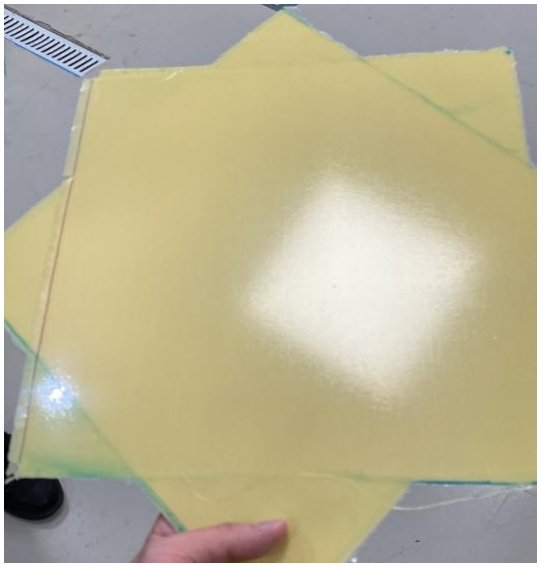

Figure 2.17. Cured top side composite, showing the finish on the part.

After the production, composites are cut into required $15\text{cm} \times 15\text{cm}$ pieces. Top composites are cut as shown in Figure 2.18.

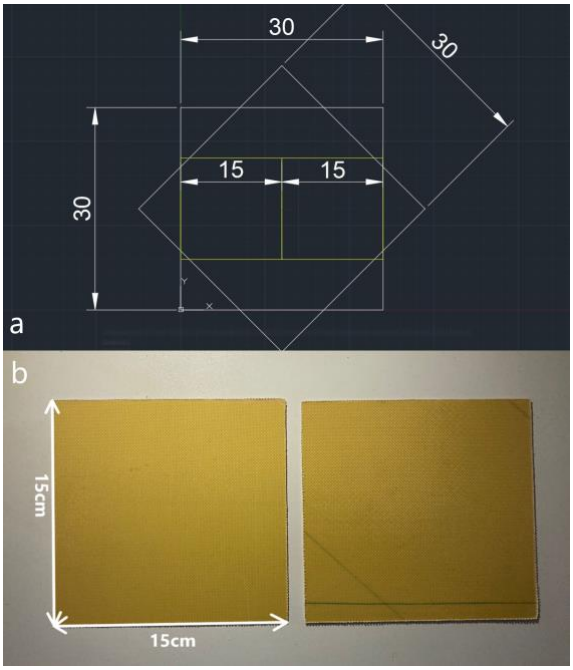

Figure 2.18. a) AutoCAD drawing, b) cut pieces

Bottom composites are already on the same $90°$ angle so they are just cut to 4 pieces. Before the assembly process, to dry the composites they are left on a stand vertically and air is blown on the composites for 24 hours. These pieces are weighed at 30g and from the density of our fabric for $15\text{cm} \times 15\text{cm}$ pieces we find a mass of 18g of fabric. This results in epoxy mass fraction ratio of 40% and fiber mass fraction ratio of 60%.

Table 2.8. Resultant characterization of manufactured composites.

Property	Value
Fiber mass (g)	18g
Total mass (g)	30g
$m_e(\%)$	40%
$m_f(\%)$	60%

On the other hand, the core structures are 3D printed on Ultimaker2 Extended printer. For one honeycomb structure the machine takes 4.5 hours and for the scutoid it is 6 hours. For 2 honeycomb and 2 scutoid cores totaling up to 21 hours.

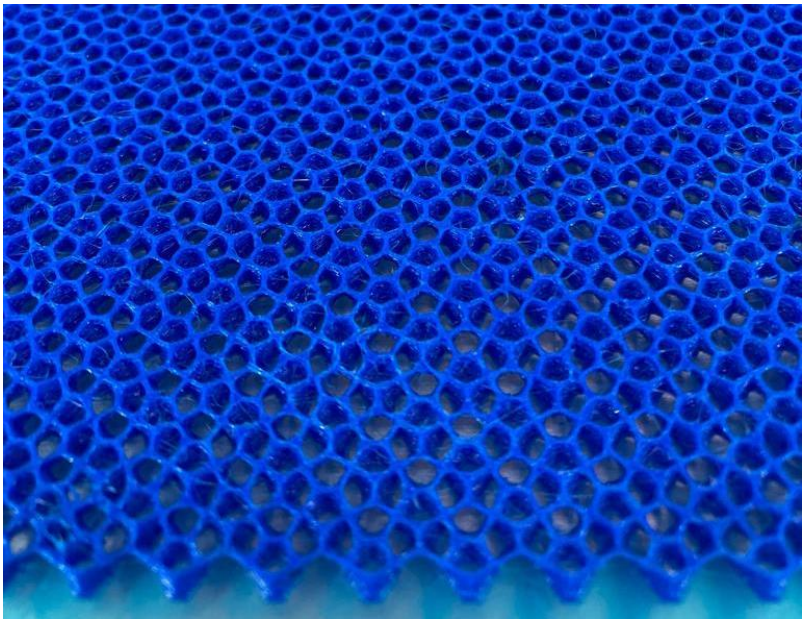

Figure 2.19. PLA scutoid core.

After the manufacturing of the parts, they are assembled using an epoxy interface. Firstly, on bottom ply epoxy is spread and core is placed on top of it. To make sure the connection is is solid, 3kg distributed load is placed on top of the core for 24 hours, and repeating the same process upside down, assembling the other composite face. This is done for 2 honeycomb, 2 scutoid and 2 plain composites totaling up to 72 hours of assembly process.

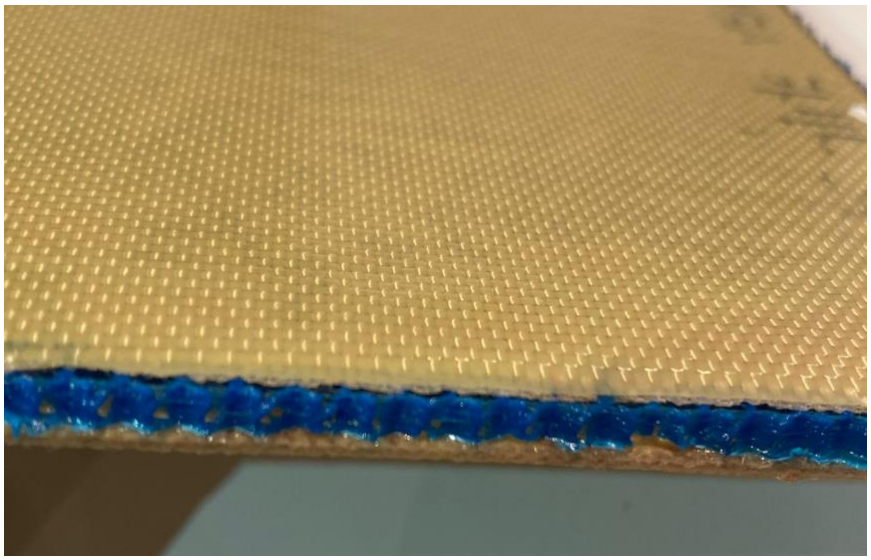

Figure 2.20. Assembled sandwich panel.

2.4.4 Low Velocity Impact Testing

After assembly, drop weight impact (DWI) tests are conducted in order to understand the improvement done on the impact absorption capability of the panel and to see the validity of the numerical studies.

LVI test are carried out according to ASTM D7136 DWI standard (ASTM, 2020) using the BESMAK BMT-DW series drop weight impact testing machine as seen in Figure 2.21 at Istanbul Technical University.

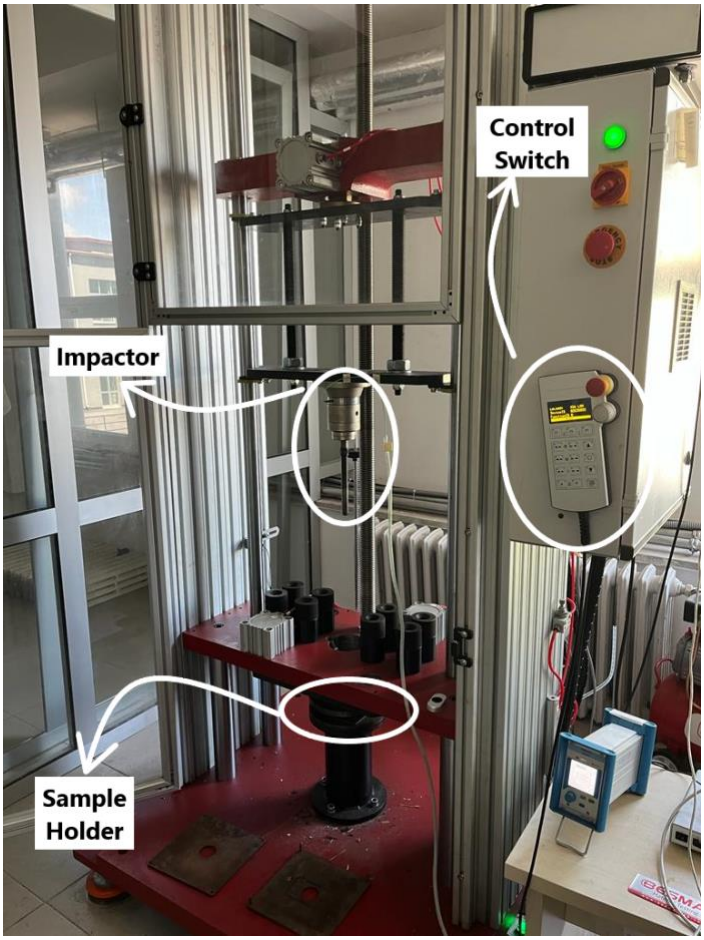

Figure 2.21. BESMAK BMT-DW test machine.

The weight of the impactor is not changeable and rated at 41kg. Numerical studies are conducted at $10\mathrm{m/s}$ and at 150J. Using the 150J and 41kg constraints, we can find the height needed with potential and kinetic energy equity.

$$h = \frac{E_k}{m_i g} \tag{1}$$

Where:

h = Drop Height of Impactor, m.

E_k = Kinetic Energy of the Impactor at impact, J.

m_i = Mass of impactor, kg.

g = Acceleration Due to Gravity, 9.81 $\mathrm{m/s^2}$.

Using equation 1 with the constraints,

$$h = \frac{E_k}{m_i g} = \frac{150}{(41)(9.81)} = 0.37293 \text{ m} = 372.93 \text{ mm}$$

Impactor is retracted to 372.93 mm above specimen and set loose. The tests that are done are shown below.

Table 2.9. List of tests conducted.

Test Type	Amount
Honeycomb Sandwich Panel	2
Scutoid Sandwich Panel	2
Aramid Composite	2
Aluminum 2024	2

2.5 Feasibility and Cost Analysis

An important aspect of a design is the cost analysis.

Table 2.10. Cost analysis of the project.

	Manufacturing Cost	Number Of Amount	Cost
Manufacturing Cost	Aluminum	$2 \times (15\text{cm} \times 15\text{cm})$	৳200.00
	PLA	-	-
	Aramid Plies	$2m^2$	৳2,663.13
	Resin	1L	৳758.00
	Hardener	340mL	
	Flow mesh	1 meter	৳139.70
	Spiral Tube	3 meters	৳80.28
	Pipe	6 meters	৳114.00
	Vacuum Resin Infusion Line Clamp	2	৳1,338.14
	T-Fitting	4	৳53.52
	Vacuum Seal Tape	15meters	৳252.91
	Peel Ply	2 m^2	৳165.92
	Vacuum Bag	7 meters	৳749.35
Industry Cost	Water Jet	6 composites	৳1,500.00
	DWI Test	10	৳2,360.00
		TOTAL	৳10,374.97

For the manufacturing the infusion machinery is not added since it is not paid for. Manufacturing cost considers the production of composite and core. The materials that are used in stock are shown with a dash.

3 RESULTS and DISCUSSIONS

Test results show us a trend of increase in absorbed energy through plain composite, honeycomb sandwich, scutoid sandwich and aluminum.

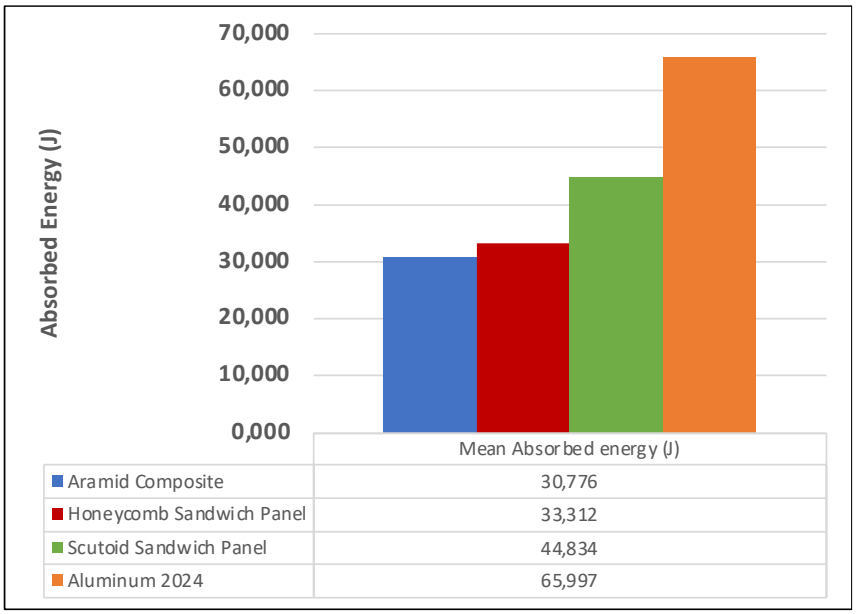

Figure 3.1. Mean absorbed energy bar graph of test results.

The trend can be seen on Figure 3.1. At this point it is important to note that the initial honeycomb data was lower than it should have been due to mismanagement of the test, so mean data does not clearly show the trend. The "should have been" trend can be seen on Figure 3.2.

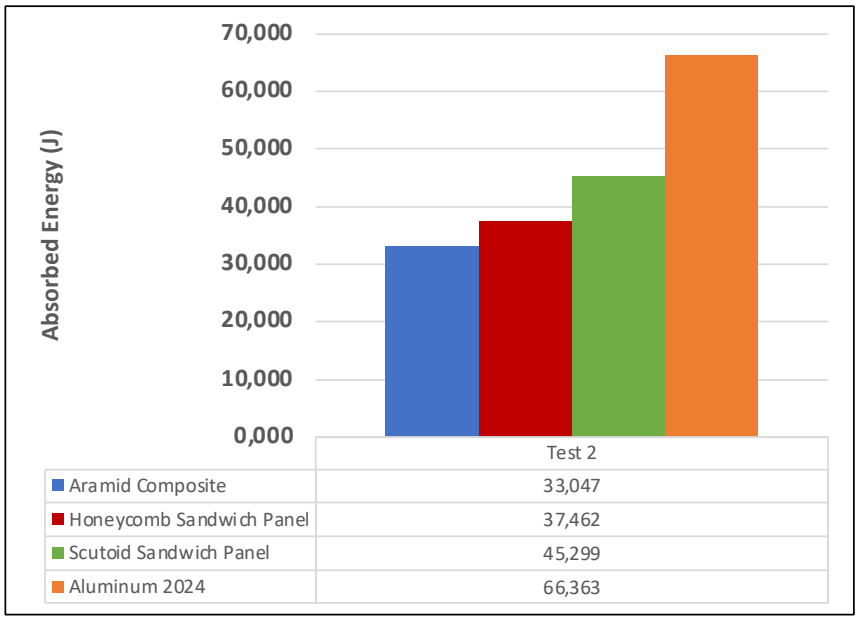

Figure 3.2. Bar graph of absorbed energy of 2nd test data.

For this reason, using the second data set is clearly a better choice. This also can be seen on the statistical values.

Table 3.1. Test results in Absorbed Energy.

Test Type	Test number	Absorbed Energy (J)	Mean Absorbed Energy (J)
Aramid Composite	1	28,504	30,776
	2	33,047	
Honeycomb Sandwich Panel	1	29,161	33,312
	2	37,462	
Scutoid Sandwich Panel	1	44,368	44,834
	2	45,299	
Aluminum 2024	1	65,630	65,997
	2	66,363	

Using these test data and the mean values if we calculate the increase in absorption rate between honeycomb and scutoid.

Table 3.2. Comparison of error based on different samples.

	Based on Second Data Set	Based on Mean Values
Increase in Absorption (%)	20,92	34,59

As we can see using different data set results in a considerable difference in increase in performance of sandwich panels. Performance of aluminum is as expected due to its enhanced properties with respect to composites. We can see that with scutoid core improvement we move a step closer to the aluminum's performance.

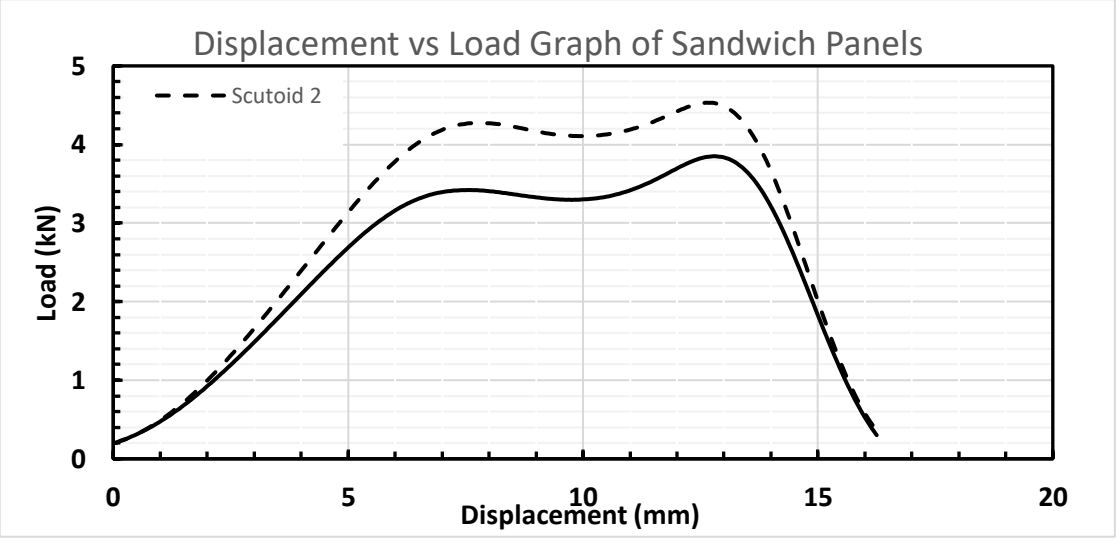

Figure 3.3. Load-Displacement graph of honeycomb and scutoid sandwich panels.

Energy absorbed is calculated automatically with the test machinery, using area under the load-displacement curve. From Figure 3.3 it is clear that scutoid line has some offset with respect to honeycomb line, making the area larger, thus more energy is absorbed in scutoid core sandwich panel.

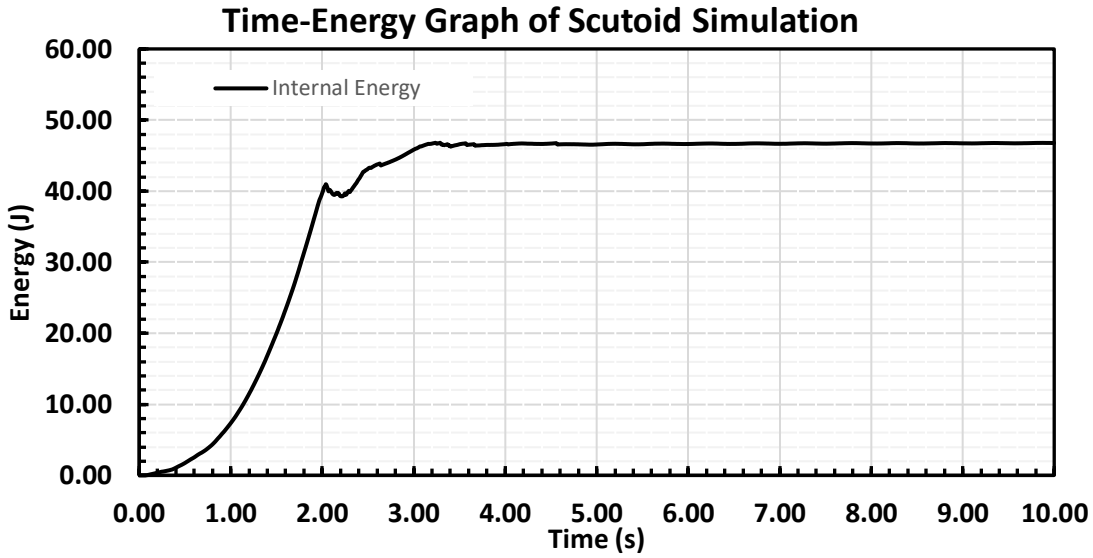

Figure 3.4. Time-Energy Graph of Scutoid Simulation taken from Ls-Prepost.

If we analyze the difference of scutoid simulation with the test results. We can see that it resulted in a closer value than honeycomb simulations. Tests results are around 44.834J and the simulation result is around 46.7J, resulting in a 4.12% error.

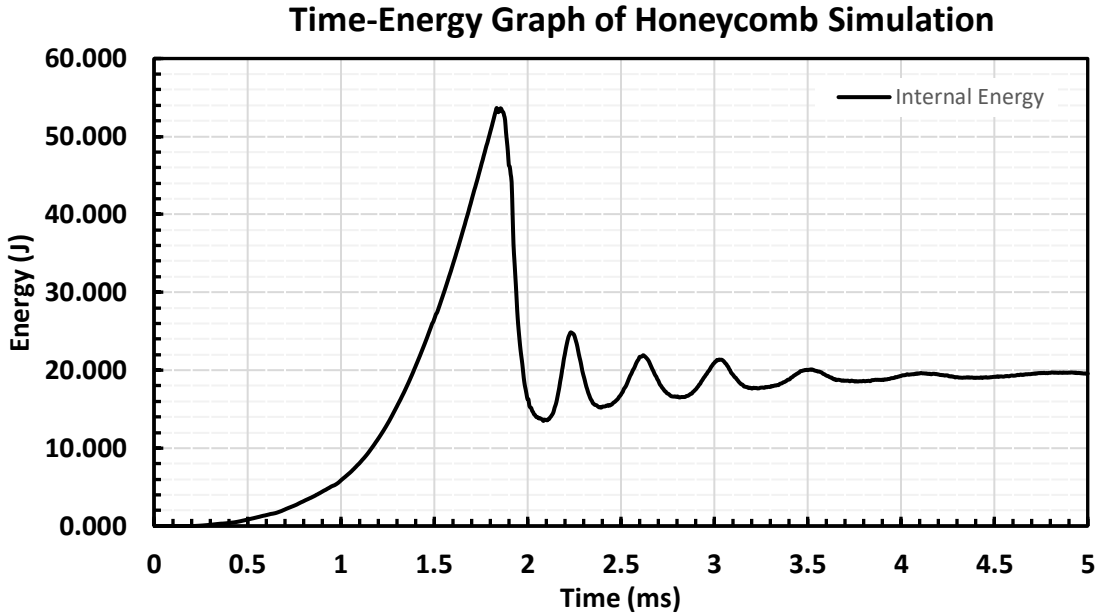

Figure 3.5. Time-Energy Graph of Honeycomb simulation taken from Ls-Prepost.

The honeycomb simulation, however, is not very consistent with the experiment results. We see that the 3D printer nozzle printed our core thickness as 0.2mm. In the first simulation were run before the manufacturing and we ran it as 0.4mm. After adjusting the value and re-running the simulation it gave us an absorption value of 53.652J, comparing with the second data results in a 43.22% error.

4 CONCLUSION and FUTURE WORK

In this undergraduate study, an innovative core geometry was analyzed by both numerical and experimental methods to design a composite panel with high impact resistance and compared with conventional core geometry and plain composite.

Ply angle optimizations were carried out with ANSYS Ls-Dyna then with optimum angles scutoid geometry were analyzed. After the composites were produced, DWI tests were carried out for validation.

Numerical studies have shown that honeycomb sandwich having, $[90]_s$ bottom and $[0/45]_s$ top laminate was the best performing sandwich panel among the other 15. Results showed that 115J of energy was absorbed by the sandwich panel. With same composites scutoid core solutions showed an absorption of 46.7J.

After the simulations, test results have shown that sandwich panels are superior to plain composite panels in terms of energy absorption. Also, the core geometry is seen as an important factor. DWI test of scutoid sandwich panel showed a close result to the simulation with energy absorption of 44.834J. This resulted in an error of 4.12%, this also shows that the second modeling approach is a better suited way to solve this problem. However, honeycomb tests showed us a value way smaller than the simulation. After seeing the results, we revised the simulation. Result of the simulation changed to 53.652J. DWI tests showing an absorption of 37.462J and resulting in a 43.22% error with our revised simulation results. We see that bio-inspired scutoid core geometry “scucomb” is also superior to traditionally used honeycomb. Scutoid core geometry absorbed 20.92% more energy, than traditional honeycomb core.

Bio-inspired scutoid core has performed better in impact resistance than traditional honeycomb core. The scutoid shape is not suitable for production using traditional manufacturing methods. As we used in this study it is likely to be manufactured using 3D printers. Making the bio-inspired designs a possible area to work at. Also, these types of new geometries can be combined with gel cores. For further work, by using genetic algorithms, the parameters of the scutoid geometry can be optimized and better performing designs can be revealed. Also, another problem we faced was to fit the scutoid shape into a complex geometry, such as, a leading edge of a wing design. New techniques can be developed for further design problems.

5 References

Abrate, S. (1991). Impact on laminated composite materials. 1.

Abrate, S. (1994). Impact on laminated composites: Recent advances. 1.

Anderson, T., & Madenci, E. (2000). Experimental investigation of low-velocity impact characteristics of sandwich composites.

ASTM. (2020, 11 2). Test Method for Measuring the Damare Resistance of a Fiber-Reinforced Polymer Matrix Composite to a Drop-Weight Impact Event. *ASTM International*. doi:10.1520/D7136_D7136M-15

Ayten, A. İ. (2020). Developement of Energy Absorbtion Capability of Present Boy Armor System by Adding Different Filler Materials and Changing Geometry. 56.

Beaumont, P., Constantinos, S., & Hodzic, A. (2015). *Structural Integrity and Durability of Advanced Composites.* Woodhead.

Cantwell, W. J., & Morton, J. J. (1991). The impact resistance of composite materials - a review. *Composites, 22*(5), 347-362.

Dhari, R. S., & Patel, N. P. (2021). *On the Crushing Behaviour of Scutoid-based Bioinspired Cellular Structures.* International Journal of Crashworthiness.

Dogan, A., & Arikan, V. (2017). Low-velocity impact response of E-glass reinforced thermoset and thermoplastic based sandwich composites. 1.

Donadon, M. V., Ianucci, L., Falzon, B. G., Hodgkinson, J. M., & Almeida, S. F. (2008). A progressive failure model for composite laminates subjected to low velocity impact damage. 1.

Farah, S., Anderson, D. G., & Langer, R. S. (2016, December 15). Physical and mechanical properties of PLA, and their functions in widespread applications — A comprehensive review. *Advabced Drug Delivery Reviews(107)*, 367-392.

He, W., Yao, L., Xiangijan, Sun, G., Xie, D., & Liu, J. (2019). Effect of structural parameters on low-velocity impact behavior of aluminum honeycomb sandwich structures with CFRP face sheets. 1.

Hosur, M. V., Abdullah, M., & Jeelani, S. (2005). Studies on the low-velocity impact response of woven hybrid composites. 1.

Huntsman. (2012, 07 25). *swiss-composite*. Retrieved from swiss-composite website: https://www.swiss-composite.ch/pdf/t-Araldite-LY1564-Aradur3486-3487-e.pdf

Irisarri, F., Lasseigne, A., Leroy, F., & Le Riche, R. (2014). Optimal design of laminated composite structures with ply drops using stacking sequence tables. *Composite Structures*, 559-564.

L K Grunenfelder, N. S., Salinas, C., Milliron, G., Yaraghi, N., Herrera, S., Evans-Lutterodt, K., . . . Kisailus, D. (2014). Bio-inspired impact-resistant composites.

Li, Z., Khennane, A., P, H., & Brown, A. (2017). Impact behaviour of pultruded GFRP composites under low-velocity impact loading. 1.

Mach, F. (2015). Reduction of Optimization Problem by Combination of Optimization. 1.

Mathivanan, N. R., & Jerald, J. (2010). Experimental Investigation of Woven E-Glass Epoxy Composite Laminates Subjected to Low-Velocity Impact at Different Energy Levels. 1.

Matthews, F. L., & Rawlings, R. D. (1994). *Compsoite Materaisl: Engineering and Science* (1 b.). England: Woodhead Publishing limited.

Naik, N. K., Sekher, Y. C., & Meduri, S. (2000). Damage in woven-fabric composites subjected to low-velocity impact. 1.

Ross, P. j. (1995). *Taguchi Techniques for Quality Engineering.* New york: McGraw-Hill Professional.

Shi, Y., Swait, T., & Soutis, C. (2012). Modelling damage evolution in composite laminates subjected to low velocity impact. 1.

Taguchi, G. (1990). *Introduction to Quality Engineering.* Tokyo: Asian Productivity Organization.

Tita, V., Carvalho, J. d., & Vandepitte, D. (2008). Failure analysis of low velocity impact on thin

composite laminates: Experimental and numerical approaches. 1.
Usta, F., Türkmen, H. S., & Scarba, F. (2021). Low-velocity impact resistance of composite sandwich panels with various types of auxetic and non-auxetic core structures. 1.
Wang, Z. (2019). Recent advances in novel metallic honeycomb structure. *Elsevier*.
Zhang, X., Xu, F., Zang, Y., & Feng, W. (2020). Experimental and numerical investigation on damage behavior of honeycomb sandwich panel subjected to low-velocity impact. 1.

APPENDICES

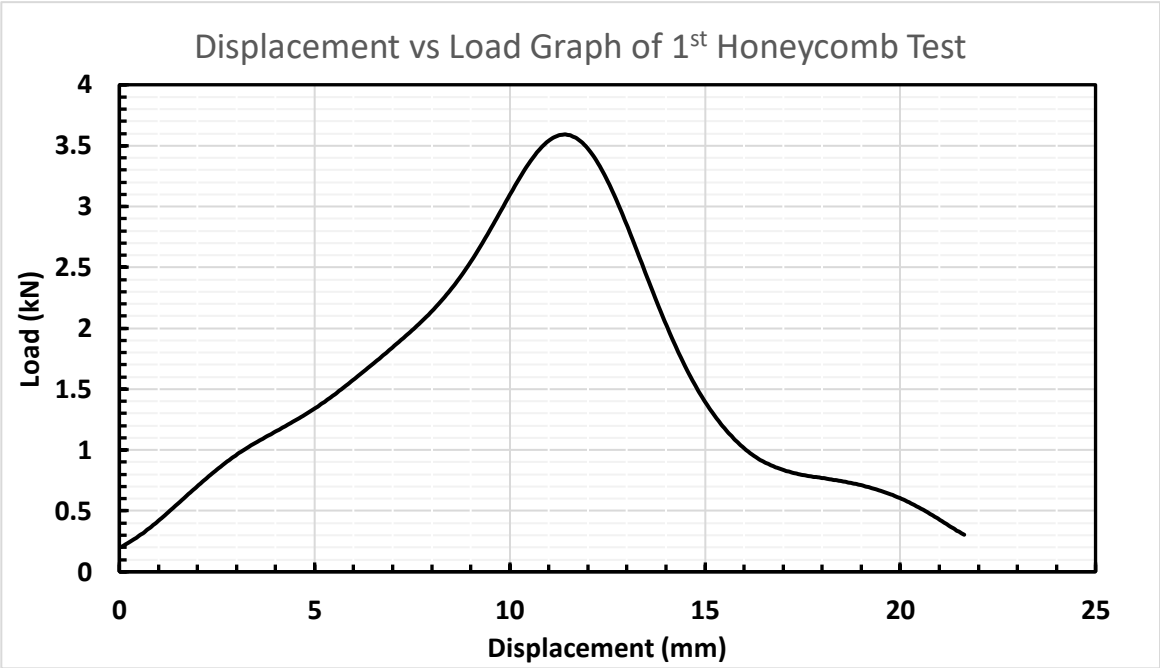

Figure 5.1. Test result of first honeycomb DWI test.

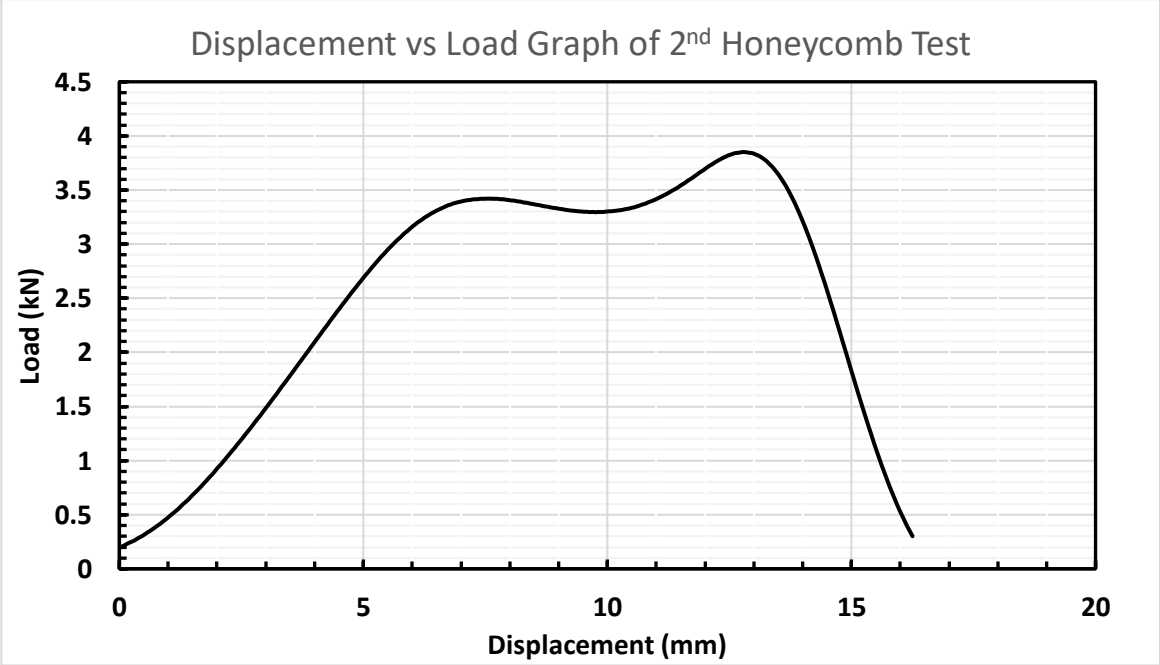

Figure 5.2. Test result of second honeycomb DWI test.

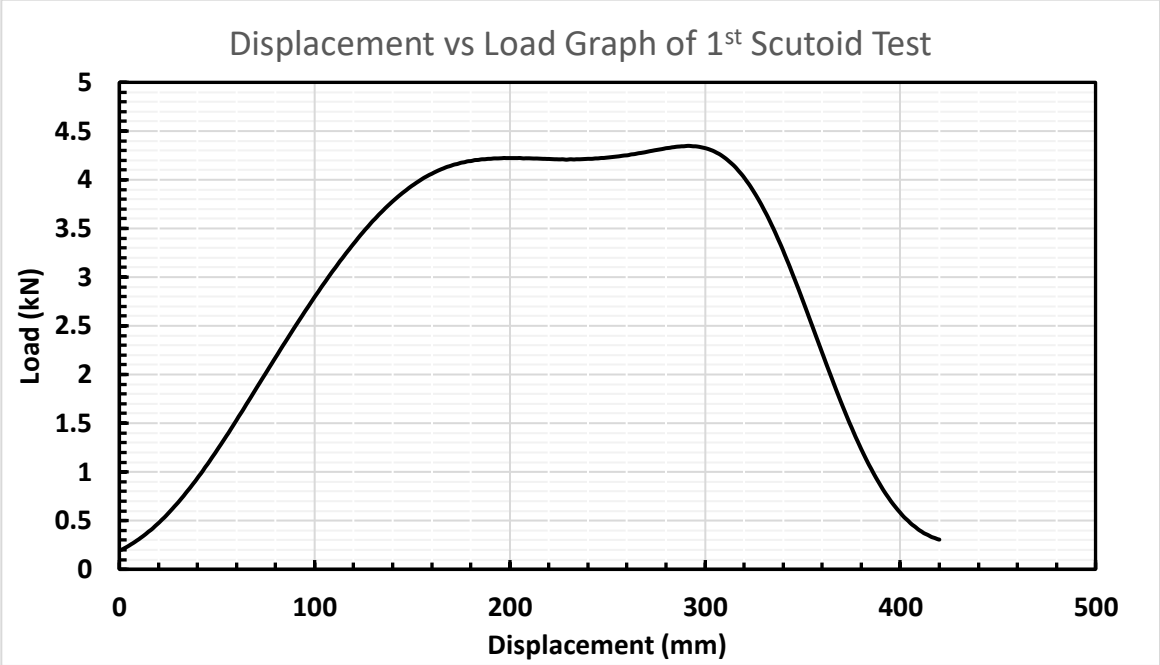

Figure 5.3. Test result of first scutoid DWI test.

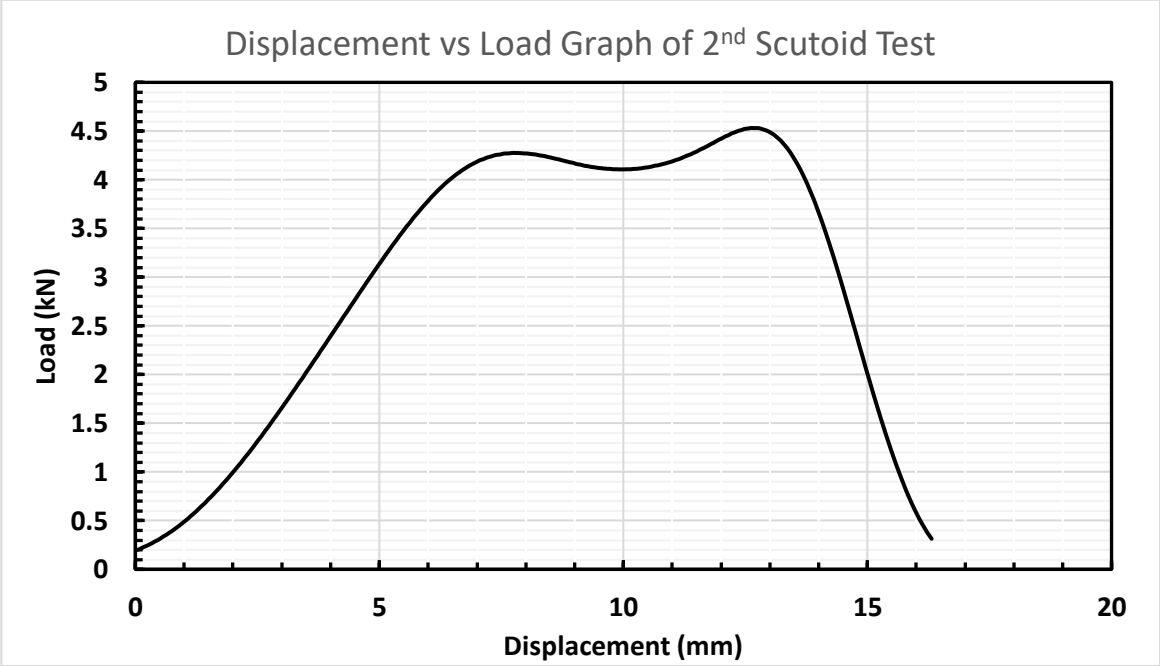

Figure 5.4. Test result of second scutoid DWI test.

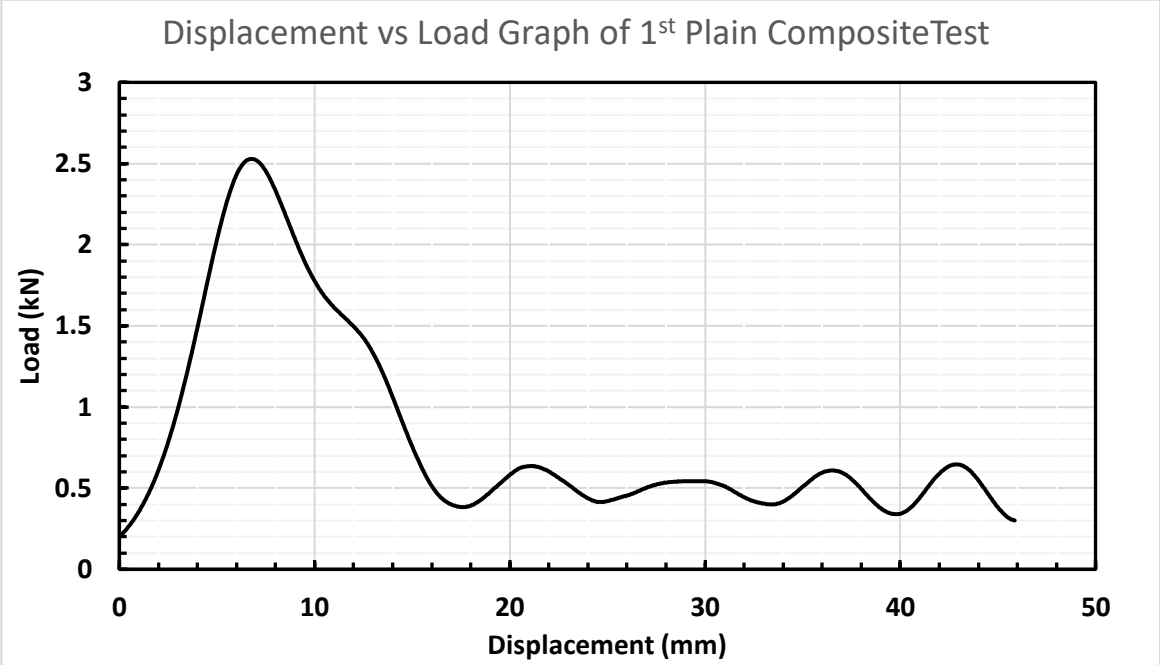

Figure 5.5. Test result of first plain composite DWI test.

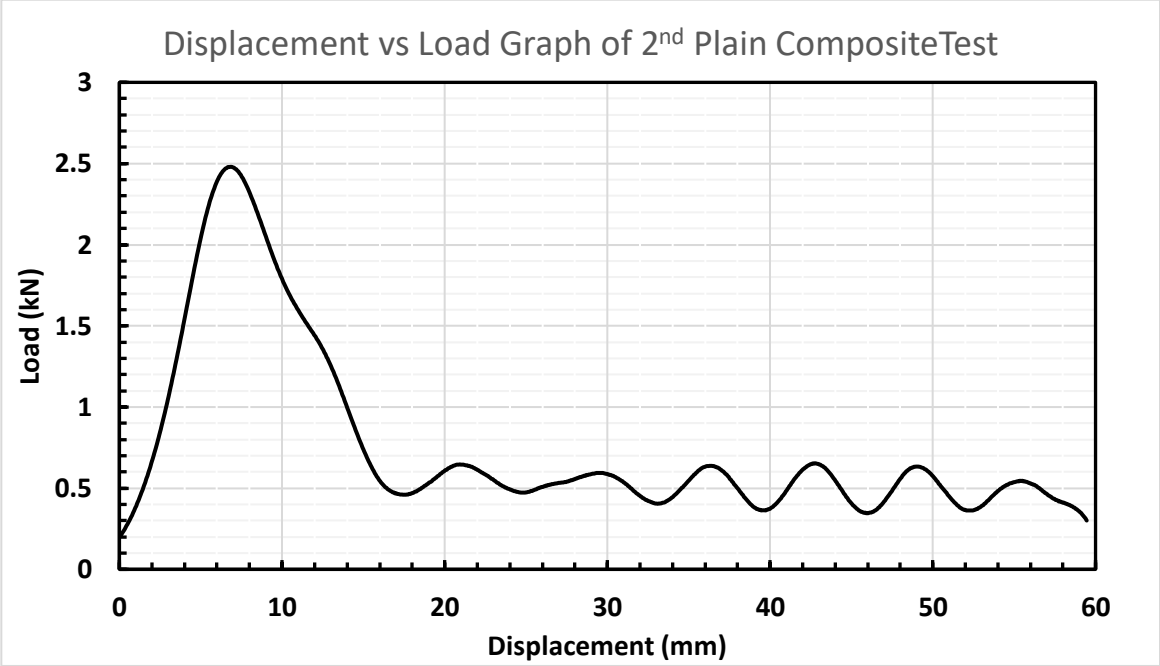

Figure 5.6. Test result of first plain composite DWI test.

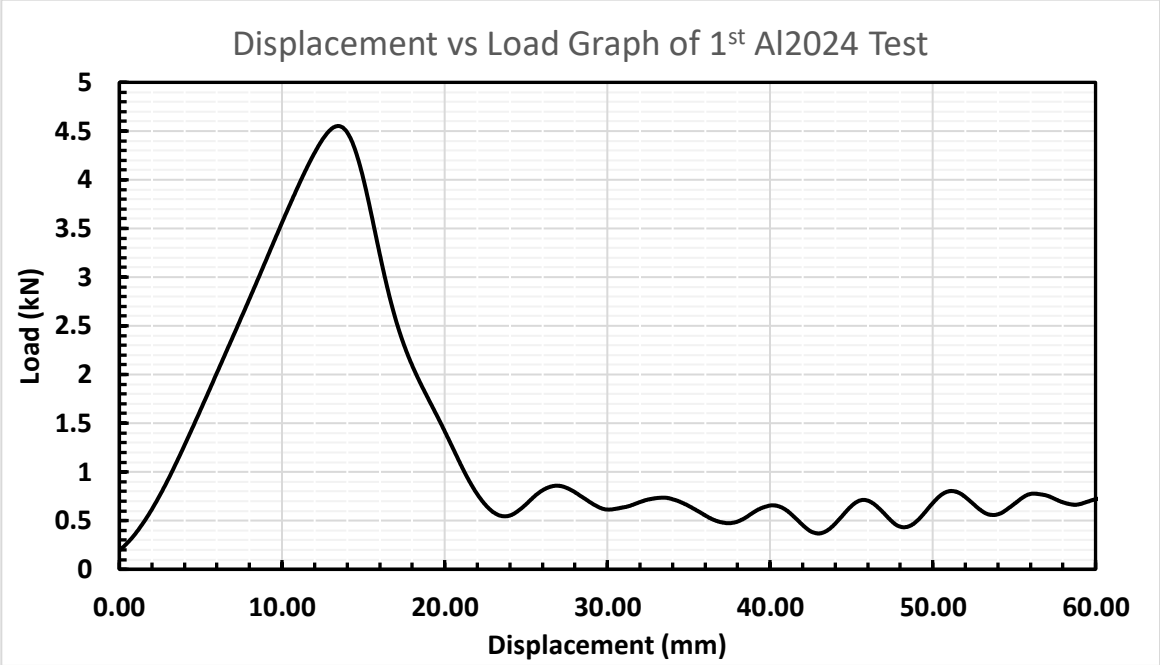

Figure 5.7. Test result of first Al2024 DWI test.

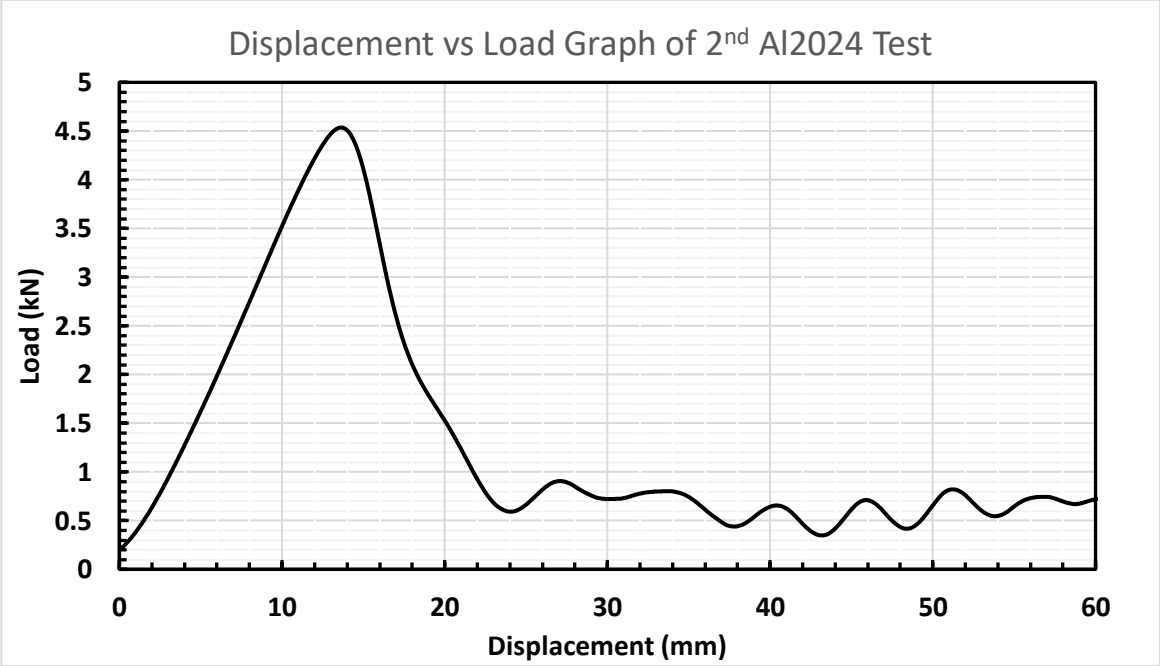

Figure 5.8. Test result of second Al2024 DWI test.

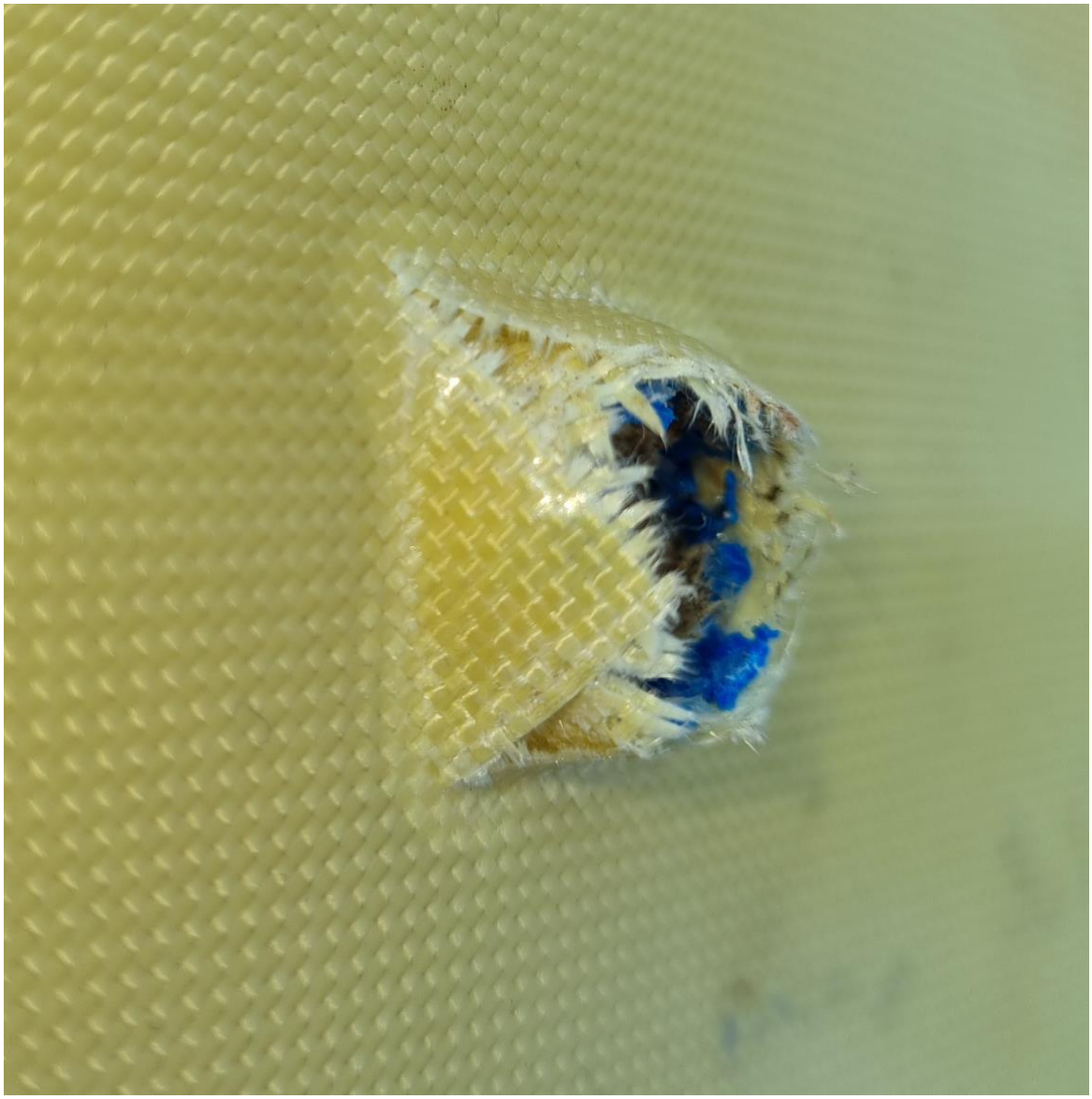

Figure 5.9 After impact image of first honeycomb impact test.

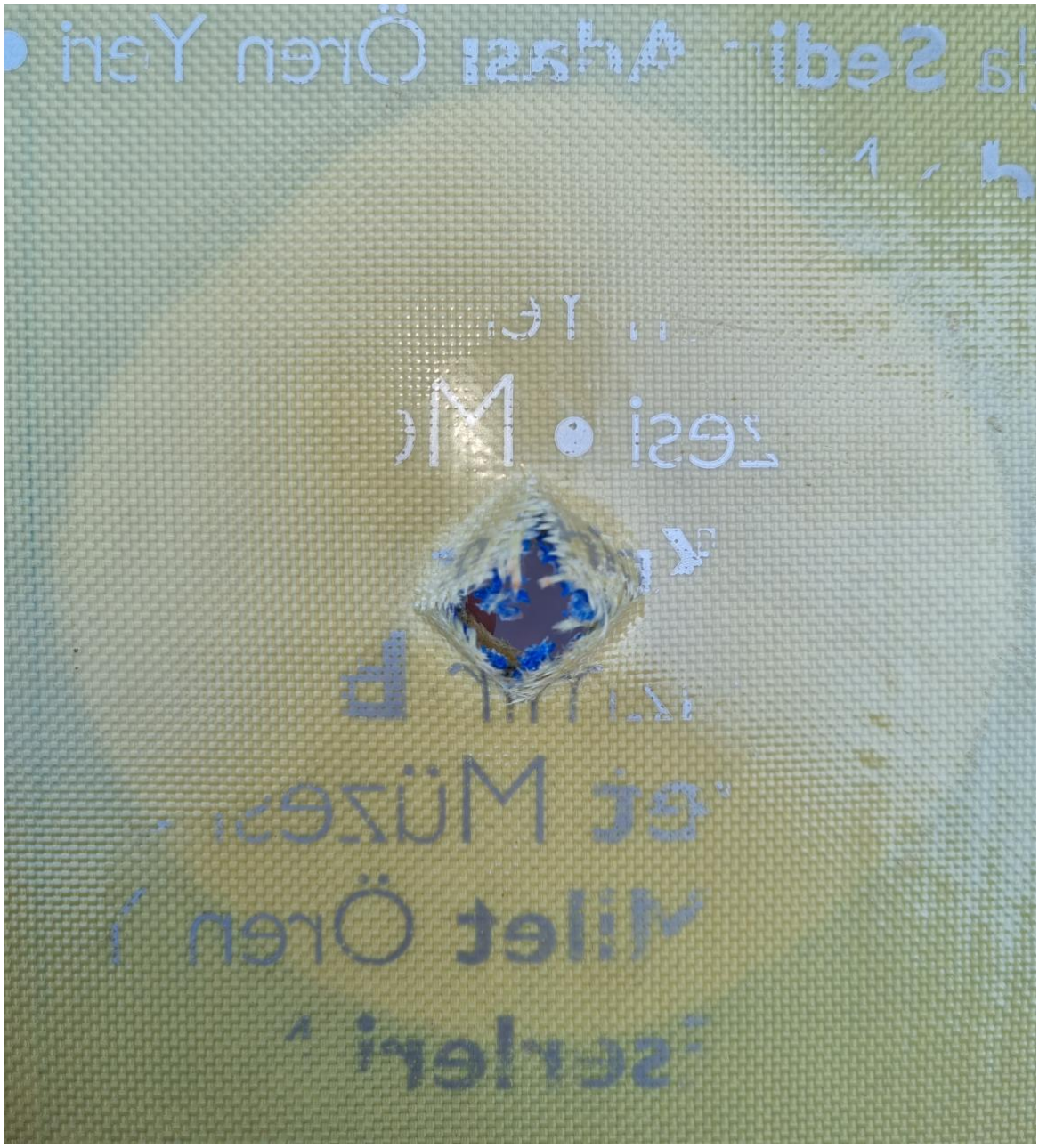

Figure 5.10. After impact image of first scutoid test. Delamination is seen.